12-2004

Thermal Modeling and Imaging of As-built Automotive Parts

Vijaya Priya Muthusamy Govindasamy
University of Tennessee - Knoxville

To the Graduate Council:

I am submitting herewith a thesis written by Vijaya Priya Muthusamy Govindasamy entitled "Thermal Modeling and Imaging of As-built Automotive Parts." I have examined the final electronic copy of this thesis for form and content and recommend that it be accepted in partial fulfillment of the requirements for the degree of Master of Science, with a major in Electrical Engineering.

Mongi A. Abidi, Major Professor

We have read this thesis and recommend its acceptance:

Andreas Koschan, Seong G. Kong

Accepted for the Council:
Carolyn R. Hodges

Vice Provost and Dean of the Graduate School

(Original signatures are on file with official student records.)

To the Graduate Council:

I am submitting herewith a thesis written by Vijaya Priya Muthusamy Govindasamy entitled "Thermal Modeling and Imaging of As-built Automotive Parts." I have examined the final electronic copy of this thesis for form and content and recommend that it be accepted in partial fulfillment of the requirements for the degree of Master of Science, with a major in Electrical Engineering.

Mongi A. Abidi

Major Professor

We have read this thesis and
recommend its acceptance:

Andreas Koschan

Seong G. Kong

Accepted for the Council:

Anne Mayhew

Vice Chancellor and
Dean of Graduate Studies

(Original signatures are on file with official student records.)

Thermal Modeling and Imaging of As-built Automotive Parts

A Thesis
Presented for the
Master of Science Degree
The University of Tennessee, Knoxville

Vijaya Priya Muthusamy Govindasamy

December 2004

Acknowledgements

I take this opportunity to thank each and everyone who stood behind me without whom I would not have come to this level of achievement in my life. I don't find words to express my gratitude to my lovable husband, Giri, who with his constant support encouraged me to purse my graduate degree. Thanks a million to him for always being there for me. I would like to express my gratitude to my grandfather Ponnusamy, my mother Manimozhi, my father Govindasamy and my sisters Geetha and Anitha for their consistent support.

I would sincerely like to thank my Professor Dr. Mongi A. Abidi, for giving me an opportunity to pursue my Masters degree under his supervision. His expertise, understanding, moral support and patience added considerably to my graduate experience. I would also like to express my gratitude to Dr. Andreas Koschan, for his expert advice and technical support which has molded my research to a good shape. Also, I would like to thank, Dr. David Page for being readily available for technical or non technical discussions. I would like to thank Dr. Seong G. Kong for serving on my graduate committee. I also extend my sincere gratitude to my friend, Ezhil Venthan who, when I had only the vaguest idea of how a car works, took the time to explain the various different processes that take place inside the car. I thank him for being so patient and spending his valuable time for me amidst his busy schedule. I would like to express my gratitude to Dr. Laura Morris Edwards for her help in polishing this thesis.

I would like to express my sincere thanks to Vicki Courtney Smith and Kim Cate for their help and support in all kind of aspects. A special thanks to Justin Acuff, who with a magic touch did miracles. Finally I would like to thank all of my friends both here in USA and back in India who has always made me feel wonderful and so special with their valuable friendship.

Abstract

Simulation is of significant importance in the automotive industry and can be done for various applications ranging from fluid flow analysis to complex thermal management of components. This thesis describes the method and necessary requirements for thermal modeling of automotive parts. Simulation of under hood and under vehicle automotive poses several challenges, the shape and complexity of the geometry used being the first and foremost to be considered. This thesis addresses the simulation of thermal images of as-built automotive parts using the 3D meshes generated from 3D modeling tools, CAD meshes and reverse engineered meshes.

Thermal modeling requires complete knowledge about the under hood and under vehicle automotive components. Many factors, both inside and outside the vehicle, affect the heat flow pattern of the vehicle under consideration. Thermal image sequences of under vehicle chassis were acquired to understand the thermal heat pattern and to serve as a basis for simulation. It was inferred that the exhaust system is the system with significant change in temperature and is at temperature close to 450 degree Celsius when the engine is operating at its full capacity. The exhaust system components, namely the catalytic converter, muffler and the exhaust pipes, were considered as the significant components for thermal modeling. The temperature curves of those components were measured with the help of an infrared thermometer to enhance the results of simulation. Application of thermal imaging in the field of threat detection is also addressed in this thesis.

Simulation or thermal modeling of the automotive components was done using the software MuSES. The thermal properties and the boundary conditions were assigned to the 3D geometry used and the transient solution was carried out over a period of time. The results for the three types of meshes mentioned earlier are presented and the thermal predictions are analyzed. As-built models can be modeled as they are with the help of reverse engineering, and the temperature predictions of those components provide better simulation results close to reality. The thesis also addresses the idea of comparison between simulation results and real time experimental results.

Contents

List of Tables

List of Figures

1 INTRODUCTION

Thermal modeling in the automotive industry consists of a host of diverse applications, which may involve a simple fluid flow on one hand, and a complex thermal management due to conduction or radiation flow on the other. The traditional design approach for almost all the automotive applications was to build prototypes and perform physical testing on them which involves the expense of time and cost. Virtual thermal modeling based on computational fluid dynamics (CFD) now complements physical testing of various automotive components and relative thermal issues and thereby minimizing the effort and cost involved in physical testing. CAD models are not readily available in a form suitable for thermal modeling and may sometimes be incomplete or may include a detail which is not required for modeling. In this thesis, thermal models of as built automotive components are simulated based on the reversed engineered (laser scanned and reconstructed) model and present an extension of comparison between real and simulated thermal images.

In the past several approaches have been made to simulate thermal signatures of under hood and under vehicle automotive parts based on computer aided design (CAD) generated meshes or meshes developed from 3D modeling tools. CAD models on their own are not best suited for thermal modeling due to unavailability of CAD models from manufacturers detailing the interior components. CAD models are not perfectly clean surface meshes and they are very voluminous. Srinivasan et al. [Srinivasan et al., 2004] describe the use of rapid omni-tree based Cartesian mesh to reduce the volume of the mesh for vehicle thermal management. Damodaran et al. [Damodaran et al., 2000] discuss the method of simulation to identify and resolve under hood and under vehicle thermal issues. Current significant areas of thermal modeling can be grouped together under the general headings of front end, under hood, underbody, external aerodynamics, air handling, passenger compartment, brake cooling and power train applications.

Virtual simulation of thermal signatures has had or can have a great impact on the design of many automotive components and processes such as the catalytic converter, pumps and fans, intake and exhaust ports, ducts and manifolds, engine cooling modules, emissions, air and oil filtration and thermal conditions. Effects of substrate preheating have been compared between the thermal modeling results and the experiments carried out by Dai et al. [Dai et al., 2004], which paves a way for comparison between real thermal images and simulated thermal images. Comparison between real thermal images and simulated thermal images poses several challenges. Modeling of as-built under vehicle automotive parts involves the generation of meshes that are the exact replica of

the component, which is not always possible with the use of CAD meshes. Another approach is the generation of 3D meshes of as-built automotive parts by reverse engineering the actual parts. Thermal images have been simulated for all the three types of meshes namely:

- The meshes created using 3D modeling tools,
- CAD meshes and
- Reverse engineered meshes.

The idea of simulation of thermal images and the challenges to be overcome to compare real thermal images with simulated ones will be discussed in detail later in this thesis.

1.1 Motivation

Simulation to date has helped to balance the management of thermal load among the under hood components and to resolve the flow problems in the under vehicle chassis. Thermal simulation of automotive parts from CAD meshes has been a popular approach mainly in the automotive industry to analyze the heat distribution and heat flow patterns in the whole car. Temperature predictions of the automotive components play a key role in thermal modeling of such parts. In this approach, thermal models are simulated based on the surface mesh and the surface temperature predicted with the help of an infrared thermometer. Thermal models developed as a result of simulation can be compared with the real thermal images of the automotive components. For comparison, the model used for simulation should be close to the real vehicle under consideration. The real vehicle can be modeled by scanning the vehicle using a laser scanner and registering the multiple views to form a single frame, which is then triangulated to form 3D mesh.

In Figure 1.1 the process of thermal modeling of under vehicle automotive parts and the visual idea of comparison between real thermal image and simulated thermal image is illustrated. It is shown that the thermal modeling of the complete under vehicle chassis involves the use of a perfect model and the assignment of thermal properties. The thermal signature prediction obtained based on the thermal properties and boundary conditions applied is then presented. Finally, the simulated thermal image is acquired based on the bidirectional reflectance distribution function, which can be compared with the real thermal image.

This research effort also emphasizes on the important application of thermal imaging in threat detection in under vehicle chassis. Low illumination and ease of reach under the vehicle sometimes fails to clearly identify the presence of threat objects in visual inspection. Thermal infrared images represent the heat energy radiated by each and every object above absolute zero.

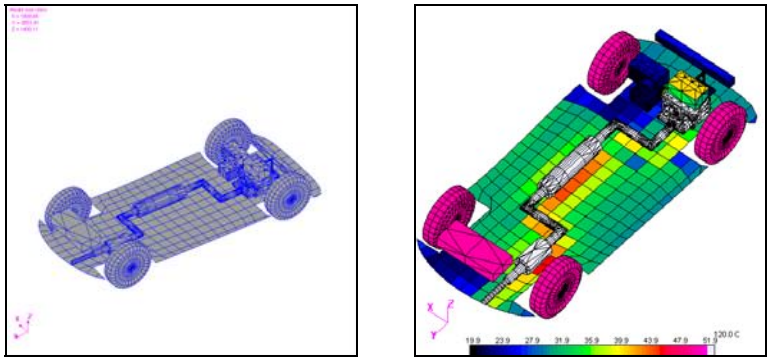

(a) (b)

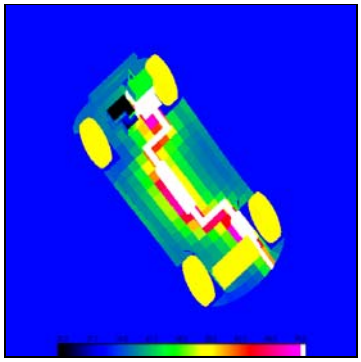

(c)

Flow of Thermal Modeling

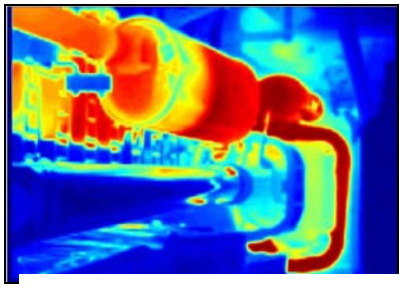

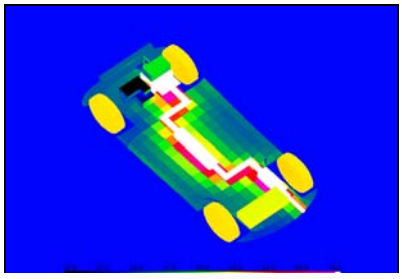

(d) (e)

Means of Comparison

Figure 1-1: Thermal modeling of under vehicle automotive components and the idea of comparison between real and simulated thermal images (a) The 3D model of the under vehicle chassis, (b – c) Simulated thermal images, (d) Real thermal image of under vehicle chassis and (e) Simulated thermal image shown here for comparison.

Threat objects like weapons, bombs and other unidentified substances placed in the under vehicle chassis can be clearly identified in the thermal scan taken underneath the vehicle. For example in Figure 1.2 the thermal scan of a car muffler with an unidentified object which is not clearly visible in the visual image is shown. The temperature of the object which is colder than the temperature of the muffler highlights the presence of the component in the thermal image.

Thermal imaging of the under hood and under vehicle automotive parts serve as a basis for thermal modeling of automotive components. Simulated thermal images can be validated by comparing with real thermal images of the corresponding vehicles. The research also highlights that the temperature curve of a particular automotive component changes with the make and model of the vehicle. For simulating thermal images of different kind of vehicles, it is necessary to have the 3D model and temperature curves of components of that vehicle.

1.2 Proposed Approach

Simulations of under hood and under vehicle automotive parts involve several challenges. One of the most significant aspects is the complexity of the geometry involved. Typical passenger vehicle under-hood is comprised of multitude of components and subcomponents. Although CAD geometry is available, clean-up of the geometry and subsequent processing to allow perfect mesh generation for thermal modeling typically involves several man weeks of CAD "clean-up" and preparation. The temperature predictions used for simulation of the models are not exact. Due to this bottleneck, engineering input from the thermal simulations was minimal in the past.

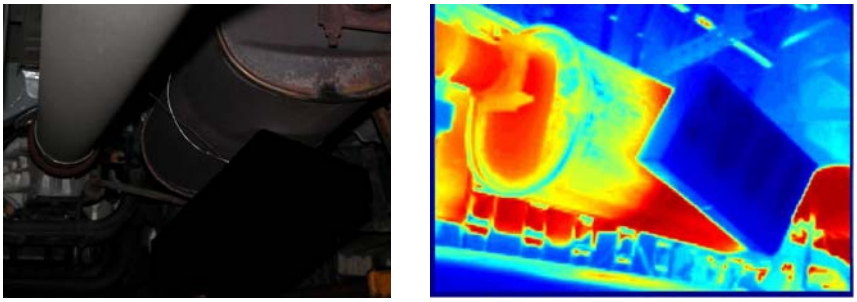

Figure 1-2: Thermal scan of muffler. The left image is a visual image of a threat object attached to the muffler. Due to low illumination, the threat object is not clearly visible. In the right image, the regular structure of the threat and its cooler temperature identifies it as an unusual object in the under vehicle chassis.

Thermal modeling of automotive components can be made close to reality by incorporating the environmental conditions, thickness, material properties and the heat flow measured for as built automotive parts. The process of temperature measurement is a dynamic experiment, which involves the time allowed for cooling of the engine before further experiments are done. Thermal image sequences captured using infrared cameras are used for validation and achieve closeness to reality.

The flow diagram of the proposed approach is presented in Figure 1.3. The work begins with the acquisition of sequences of thermal images of under vehicle chassis using infrared camera and temperature curves of automotive parts using the infrared thermometer, which serves a ground truth for validation. Thermal images were acquired using the Omega infrared camera from Indigo Systems [Indigo]. Temperature curves measured are the surface temperatures of the automotive components under consideration. The thermal properties and the boundary conditions along with the temperature curves serve as input to the signature prediction software Multi Service Electro Optic Signature (MuSES). The geometry, (self created 3D meshes or CAD meshes or reverse engineered mesh) is imported and the thermal properties are assigned. The transient analysis is done for a particular period of time, and the convergence is governed by the tolerance limit set. The radiosity solution is done for a particular wave band and the thermal image is simulated based on the bidirectional reflectance solution.

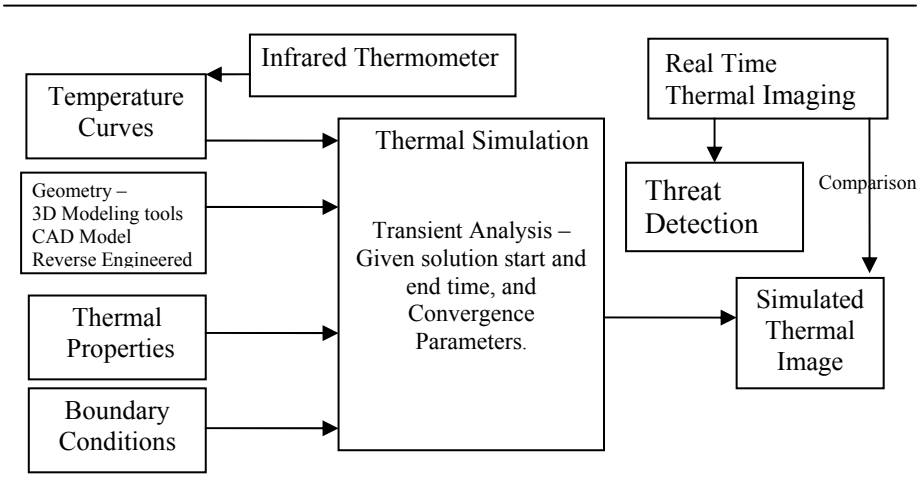

Figure 1-3: Schematic representation of pipeline of thermal simulation.

This thesis investigates the experimental achievability and limitations of thermal imaging for both data simulation and real world data acquisition. The research integrates the software and hardware tools available for experimentation, describes the simulation of automotive components, and investigates the comparison of that simulated data to actual thermal data.

1.3 Document Organization

The remainder of this thesis is organized as follows. Chapter 2 reviews the theoretical background on thermal imaging, thermal imaging systems, calibration of thermal imagers and the method of temperature measurement. The need for simulation and the concept of simulation of thermal images is presented in Chapter 3. Chapter 4 presents the experimental results of thermal data acquisition process for aiding in thermal modeling and to highlight the most important application of thermal imaging in the field of threat detection. The results of thermal modeling of automotive components are in Chapter 5. Next, Chapter 6 discusses about the requirements and challenges for comparing real time and simulated thermal images. Finally, the thesis concludes with ideas for the extension of this research in Chapter 7.

2 THERMAL IMAGING

This chapter gives an introduction to thermal imaging principles and also discusses the thermal data acquisition process. Section 2.1 gives a brief introduction to thermal image processing and talks a little about the thermal imaging device types. The calibration techniques currently in use are discussed in Section 2.3. Finally, Section 2.4 discusses the temperature measurement processes.

2.1 Thermal Infrared Fundamentals

Thermal imaging is the quantification and recording of the surface temperature of objects by non-contact sampling and analysis of the infrared emissions from that surface. Thermal images are unique for each object. Thermal imagers can see almost all objects, because all objects that do not radiate energy in the visual band radiate infrared energy that is nothing but heat energy which is produced by the motion of molecules [Zissis, 1975]. In thermal imaging, the main form of energy under consideration is called *heat*. Heat is the form of energy that is transferred from one place to another as a result of temperature difference. There is an important distinction between a thermodynamic analysis and a heat transfer analysis. Thermodynamics deals with a system at two different states of equilibrium and determines the energy exchange in going from one state to another. Heat transfer, on the other hand, deals mainly with the rate of heat transfer or the time it takes for the heat transfer to occur. Heat is the energy that an object has because of the motion of its molecules, which are continuously jiggling and moving around. When energy is added to an object, its molecules move faster, creating more heat.

Compared to a warm object, the molecules in a cold object have less molecular motion. Heat is the total energy of molecular motion in a substance. Heat can be transferred from one place to another by three methods: conduction in solids, convection of fluids (liquids or gases), and radiation through anything that will allow radiation to pass. The method used to transfer heat is usually the one that is the most efficient. For example, assume that a certain amount of air with a known temperature and flow rate enters a duct (or a pipe) [MuSES], and the air is heated as it travels through the duct, and exits at the other end. Law of conservation of energy states that the energy of the air at the exit is equal to its energy at the entrance plus the amount of energy added to it during its travel through the pipe, or

Total energy entering the system (Q_{in}) – Total energy leaving the system (Q_{out})= Change in the total energy of the system (ΔQ)

$$Q_{in} - Q_{out} = \Delta Q \tag{2.1}$$

Thermal imaging captures the infrared emissions from a particular surface and converts the radiation into an electrical signal. This data is compiled by a computer into a thermal image.

A thermal image scanner (or camera) measures infrared energy (heat) radiated from a target body, accurately converting it to thousands of equivalent temperature readings. A computer program assigns particular temperature ranges a particular color, and then displays the new colorized temperature readings as a color image, which is a thermogram or thermograph.

On a thermogram, whites, reds and yellows typically represent the warmer end of the temperature range being displayed. Blacks, blues and greens generally represent the cooler end of the same range.

Infrared radiation [Sprio, 1990] lies between the visible and microwave portions of the electromagnetic spectrum. Infrared waves have wavelengths longer than visible and shorter than microwaves, and have frequencies which are lower than visible and higher than microwaves. Infrared is broken into three categories: near, mid and far infrared. Near infrared refers to the part of the infrared spectrum that is closest to visible light and far infrared refers to the part that is closer to the microwave region. Mid-infrared is the region between the near and far infrared regions. Far infrared waves are thermal, represent the heat radiated from any object, and are quite useful in the surveillance industry which aids in viewing the target even in the absence of sufficient and/or no illumination.

In infrared astronomy, we measure heat, which has traveled by radiation. Infrared radiation (also called heat or thermal radiation) is a type of electromagnetic radiation (or light). Radiation is a form of energy transport consisting of electromagnetic waves traveling at the speed of light. Temperature is a measure of the average heat or thermal energy of the molecules in a substance. Temperature defines the state of energy within a given body and thermal radiation is described as a wave motion which follows the fundamental equation:

$$\lambda \nu = c \tag{2.2}$$

where λ represents wavelength, ν represents frequency, and c represents velocity. The spectral distribution of radiation varies with the wavelength and can be characterized

based on its distribution with wavelength λ. Sources of radiation can be continuous and smooth functions of wavelength, or can be discrete with radiation in bands.

Radiating sources can be classified as blackbodies or gray bodies. A blackbody absorbs all the radiation it receives and radiates more thermal radiation for all wavelength intervals than any other mass of the same area and temperature. Gray bodies are the ones which absorb a fraction of the radiation incident upon them. Emissivity is defined as the ratio between the radiant energy of an object and the radiant energy of a blackbody with the same temperature as the object. Emissivity ranges between 0 and 1 depending on the dielectric constant of the object, surface roughness, temperature, wavelength, viewing angle etc. Perfect blackbodies have an emissivity of 1 whereas the other radiators have an emissivity between 0 and 1.

No ideal blackbody exists in practice; specially constructed laboratory sources emit radiation with efficiency compared to a blackbody of 98% or higher. The blackbodies are commonly [Merritt et al., 1959] realized by using a spherical cavity with a small hole in the surface or a closed end tube that is longer than its diameter, shown in Figure 2.1. The opaque walls of the sphere or tube are maintained at uniform temperature. These blackbody constructions provide multiple reflections of any radiation entering the opening. After many reflections, all the energy is absorbed, and at room temperature the aperture appears to be black in the visible spectrum and totally absorbing in all other parts of the spectrum. At any given temperature, the aperture radiates energy at nearly the same rate as a blackbody of the same size and temperature.

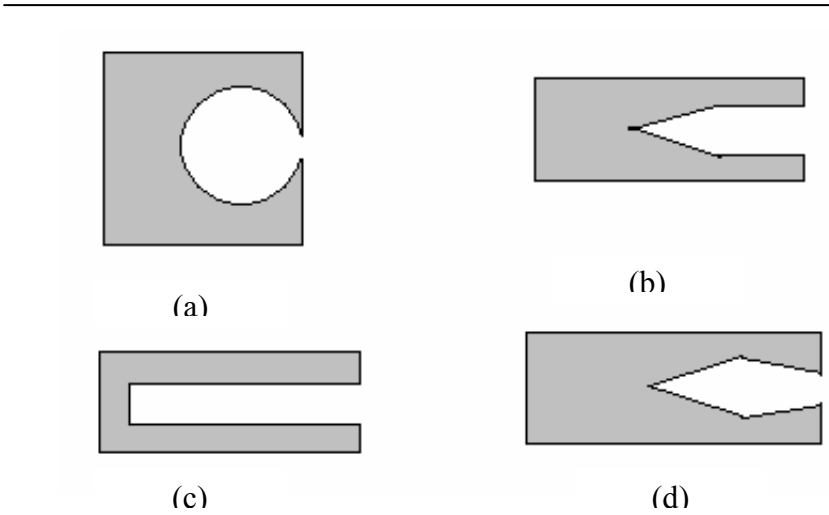

Figure 2-1: Blackbody cavities available commercially (a) Spherical (b) Conical, (c) Cylindrical and (d) Inverse Conical.

The rate at which a blackbody radiates energy is given by the Stefan-Boltzmann Law:

$$w = \sigma T^4 \tag{2.3}$$

where w = watts/meter^2, σ = Stefan-Boltzmann constant 5.6697 x 10^{-6} watts/m^2 -T , T = Absolute temperature Kelvin

The Wien-Planck law expresses the radiation emitted per unit area of a blackbody as a function of wavelength, λ, and temperature T

$$J_{\lambda T} d\lambda = C_1 \lambda^{-5} (\varepsilon^{C_2/\lambda T} - 1)^{-1} d\lambda \tag{2.4}$$

where C_1, the first radiation constant = 3.7415 x 10^{-16} watts/m^2 and C_2, the second radiation constant = 1.43879 x 10^2 meter . Kelvin

When the temperature of a blackbody radiator increases, the amount of radiation per unit area increases and the peak of the radiation curve shifts to shorter wavelengths.

Wien's Displacement Law gives the value of the wavelength of maximum radiation per unit area

$$\lambda_m T = b \tag{2.5}$$

where λ_m is the peak wavelength in meters, T is the temperature of the blackbody in Kelvin, and b - 2.8978 x 10^{-3} meter . Kelvin

Commercial blackbody calibrator sources come in different sizes and capabilities. They represent the ideal blackbody sources with high emissivities. There are certain factors which affect the purchase of the blackbody calibrators other than the temperature range.

1. Type of blackbody - Basically there are two different types of blackbody sources: the hot plate blackbody source and the cavity-type blackbody source. The hot plate consists of a metal plate, temperature controller components and the emissivity is typically 0.95. The cavity-type blackbody source consists of a blind hole in a cylinder or a sphere and the temperature is controlled using a thermocouple probe. The emissivity is high compared to hot plate source and is typically 0.98 or higher. Having a higher emissivity value increases the precision of calibration.

2. High emissivity – The higher the emissivity, the higher the cost of the blackbody. Emissivities are often measured in 9's (two 9s means an emissivity of 0.99x, three 9s means emissivity of 0.999x, where x is an integer less than 9). This is an

important factor because a small emissivity error can be translated into a radiance error in calibration.

3. Grayness - This is the uniformity of the blackbody's spectral emissivity with the wavelength. This is an essential feature because it helps in using the blackbody in many different wavebands.

4. Entrance aperture diameter - The target area should be larger than the field of view of the camera; otherwise the resulting image will include unwanted background temperature changes.

5. Response time - This is the time spent waiting for the source to stabilize at a new temperature after a change in setting, prior to testing.

2.2 Thermal Imaging Devices

Thermal imaging devices are a combination of optics, detectors and signal processing units, which detect the thermal infrared radiation emitted by the objects in the scene with out the use of artificial illumination [Chevrette, 1986]. Figure 2.2 shows the basic components of a thermal imaging device. The thermal imaging system views the target or the scene through the infrared detecting lens system which is focused on a detector array and then processed through the signal processing unit, which is finally displayed as a temperature pattern on the display system. There are two main types of thermal imagers namely the cooled thermal cameras and the uncooled thermal cameras.

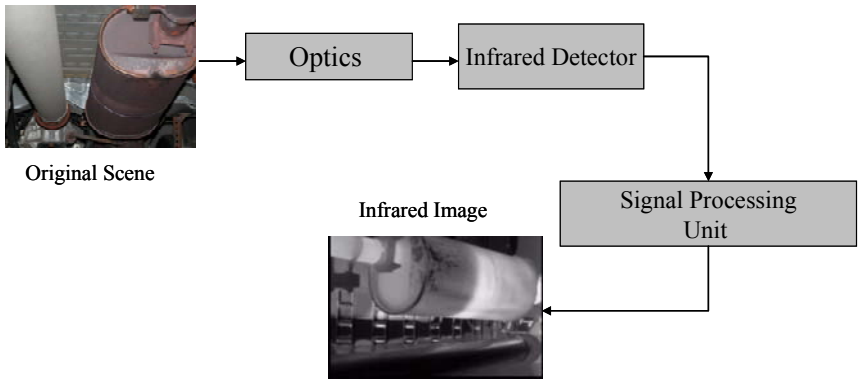

Figure 2-2: The basic components of a thermal imaging system.

Uncooled - This is the most common type of thermal imaging device. The infrared-detector elements are contained in a unit that operates at room temperature. This type of system is completely quiet, activates immediately and has a built-in battery.

Cryogenically cooled - More expensive and more susceptible to damage from rugged use, these systems have the elements sealed inside a container that cools them to below 32° F (zero C). The advantage of such a system is the incredible resolution and sensitivity that results from cooling the elements. Cryogenically cooled systems can "see" a difference as small as 0.2° F (0.1° C) from more than 1,000 ft (300 m) away, which is enough to tell if a person is holding a gun at that distance.

Thermal imaging systems work as described below

1. The lens collects the energy from a spot on the target and focuses it on the surface of the infrared detector.

2. The focused light is scanned by a phased array of infrared-detector elements. The detector elements create a very detailed temperature pattern called a **thermogram**. It only takes about one-thirtieth of a second for the detector array to obtain the temperature information to make the thermogram. This information is obtained from several thousand points in the field of view of the detector array.

3. The thermogram created by the detector elements is translated into electric impulses.

4. The impulses are sent to a signal-processing unit, a circuit board with a dedicated chip that translates the information from the elements into data for the display.

5. The signal-processing unit sends the information to the display, where it appears as various colors depending on the intensity of the infrared emission. The combination of all the impulses from all of the elements creates the image.

The infrared detector in the thermal imaging system is an important component which detects the emitted radiation and converts it into an electric signal. The infrared thermometer operates with the same principle except for the detectors. It has a point sensing instrument, which is considered to be a single channel in a large multi detector mosaic of channels that compromise focal plane array (FPA)-based thermal imagers.

The focal plane array (FPA) is the optical focus point where the image is focused. The focal plane array is made of either linear arrays of pixels or two-dimensional arrays. In an FPA, not the entire surface of the detector is sensitive to IR energy. Around the rows and columns of individual IR detectors making up the array is an inactive region surrounding

each of the detectors. The inactive areas can serve as pathways for electronic signals. The inactive regions are called the read-out integrated circuit (ROIC). The ROIC includes the means to electrically address the pixels sequentially. The ROIC sometimes embeds the signal processing units, such as amplification, signal integration, multiplexing, and analog to digital converters.

The infrared detectors exhibit some electrical change as response to the radiant energy incident on their sensitive surfaces. The change could be an impedance change, or a capacitance change, or the generation of voltage or the release of photons based on the type of detectors used. Detector response times could be as fast as nanoseconds or as slow as a fraction of seconds.

The two main types of commercially available infrared detectors are photon detectors and thermal detectors. The output of the photon detectors is governed by the rate of absorption of photons and not dependent on the photon energy. These detectors are used in the cooled infrared imagers, and must be cooled to cryogenic temperatures, by means of cryogenic solids and liquids, mechanical refrigerators, and thermoelectric coolers, in order to avoid the excessive dark current. These detectors are normally expensive but provide higher detection capabilities and slower response times.

In contrast, thermal detectors operate in a two step process. The absorption of infrared radiation in these detectors raises the temperature of the device, which in turn alters some temperature dependent parameter such as electrical conductivity. The main advantage of thermal detectors is that they operate at room temperature and avoids the artificial means of reducing temperature of the infrared array. However, the sensitivity is lower and the response time is longer than for photon detectors.

The classes of infrared detectors and the mechanisms that are used to achieve these thermal detectors are discussed by Kaplan et al. [Kaplan et al., 2001] and also a quick reference chart is provided by summarizing the commercially available thermal imager capabilities and suitable applications.

The thermal detector is divided into three functional parts, namely:

1. Absorber for infrared radiation
2. Membrane or other structure for achieving thermal insulation
3. Temperature detector

The absorber is generally a finely subdivided metal. In order to obtain high sensitivity it is important that the detector element is thermally insulated from the detector ROIC. Thin membranes are made around the thermal arrays using micro-mechanical processing techniques. The temperature detector is usually integrated into the membrane and is utilized to detect the minute temperature change resulting from the infrared radiation exposure and absorption. A brief introduction to infrared theory and thermal image

processing is given in this section. The next section discusses the characterization of the infrared detectors in the focal plane array and calibration of the complete system.

2.3 Calibration of Thermal Imaging Devices

Characterization of thermal imaging cameras is a necessary process in identification of the temperature value represented by the varying pixels in the thermal image acquired. A brief description of the techniques and methods available for thermal camera calibration is given first and a general calibration technique is described, which can be used for basic characterization of all the thermal imagers in use with the knowledge of certain parameters.

Survey on Calibration of Thermal Imaging Devices

In this section we present a review of the techniques and methods available for calibration of thermal imagers. All the methods discussed here hold well for cooled thermal cameras, which are more stable and are not easily affected by the raise in temperature. The infrared imaging sensors measure the energy radiated from the object whose temperature is being measured. The infrared image of a particular automotive part will have variations even if there are slight variations in the wavebands. Hence, calibration of a thermal image is necessary. It also aids in understanding the temperature ranges represented by various gray values or corresponding color vales in a color coded image. A general understanding of infrared technique, blackbody sources, temperature measurements and calibration of thermometers and other thermal imaging devices are obtained by reviewing [Spiro, 1990], [Quinn, 1983], [Nicholas et al., 1994] and [Jacobs, 1996].

The calibration principle described can be used for cooled thermal cameras where the resulting thermal image is not affected by system parameters and other factors. The measured temperature tends to vary over the entire image in an uncooled camera output and is not homogeneous through out the image. Hence, calibration can be effectively established for uncooled thermal cameras.

The instruments to be calibrated must be qualified in four independent domains, namely, the field of view, spectral band pass, time and polarization [Wyatt, 1976]. The paper defines the general objective of calibration as to obtain an inferential relationship of the remote source in terms of the incident flux and the instrument output

$$\begin{aligned} \phi &= f(output) \\ \phi &= \Gamma(1/R) \end{aligned} \tag{2.6}$$

where ϕ is the magnitude of radiant entity
R is the complete characterization of all four domains

The revised objective says that the calibration should be conducted under conditions which reproduce, as completely as possible, those conditions under which the measurements are to be made. The functional parameters of calibration are defined as follows

- Noise – This parameter defines the extent of error associated with any measurement

- Linearity – This parameter is measured as a relationship between source area and instrument output

- Spatial response – The goal of measurement of a radiant source, with respect to spatial parameters, is to obtain a measure of the total flux in a small region about the optical axis of the instrument

- Temporal response – The measurement goal with respect to time, is to obtain a measurement of the flux at a specific time (or as a function of time) or as a function of position (in time) for moving targets or instruments

- Polarization response – The goal is to obtain a characterization of the polarization of the source, or to ascertain if the measurement is polarization dependent

- Spectral response – This parameter obtains a measure of the total flux in a specified region about the center wavelength

Calibration loads (hot or cold) are developed for the purpose of calibration of a particular radiometer. A hot calibration load whose temperature can be measured and controlled is developed for calibrating the microwave radiometer [Xiao, 2000]. This paper concludes that the brightness temperature is a function of the angle of view. The construction of the calibration is load is described and the measurements reveal that the brightness temperature is the function of angle of view and the effect of insulation layer cannot be neglected.

Two mathematical models are applied, namely, the incoherent model, which ignores the effect of insulation layer, and the coherent model, which includes the effect of insulation layer, for the measurement of brightness temperature. The measurement of brightness temperature for this load is discussed in [Xia0, 2001]. This paper describes the DVRT (Vector radiative transfer theory of densely distributed random discrete scatters) model to calculate the brightness temperature emitted by the radiometer calibration load presented in [Xia0, 2000]. There are four cases which lead to the variation of radiative intensity: 1) the loss for the absorbing and scattering of scatters, 2) the loss for the absorbing of background, 3) the contribution of thermal emission source and 4) the contribution of

multiple scattering. The brightness temperature emitted by the calibration load is given by

$$\overline{T}_B(\theta) = \frac{1}{C} t_{10}(\theta) \begin{bmatrix} I_v(\theta, z=0) \\ I_h(\theta, z=0) \end{bmatrix}, \tag{2.7}$$

where $\overline{T}_B$ is the brightness temperature, θ is the angle of view, C is a constant, and I_v and I_h are the vertical and horizontal components of the electromagnetic field.

The conclusion states that ignoring the multiple scattering of insulation layer overestimates the thermal emission of calibration load at millimeter wave band. It is shown that when the working frequency is a constant, the DVRT brightness temperature is smaller than that of the incoherent model which proves the overestimation in the incoherent homogeneous model. For smaller fraction of scatters, the difference between the DVRT temperature and the incoherent temperature is high whereas for large volume of scatters the difference is low.

A new method is presented by Heijden et al., [Heijden et al., 2003] for automatic correction of distortions and for spectral calibration (which band corresponds to which wavelength) of spectral images. This method uses a bar-like pattern with an illumination source with spectral bands and incorporates the prior information of the wavelengths of these spectral bands and the spatial arrangement of the bars, to construct a template image whose spectral axis is linearly related with wavelength. A grid is then posted on both the recorded and template image. A penalized likelihood method in a quasi-Newton iterative optimization technique is used to shift the points in the grid of the recorded image such that the transformed image has a high resemblance (likelihood) to the template image and a low distortion (penalty term).

A simple algorithm that computes the radiometric response function of an imaging system from images of an arbitrary scene taken using different exposures is described in [Mitsunaga et al., 1999]. In brightness images, the brightness measured is assumed to be linearly related to the scene radiance. But there exists a non-linear mapping between scene radiance and measure brightness. This mapping is referred as radiometric response function of the imaging system [Mitsunaga et al., 1999].

The image irradiance E is related to scene radiance L in a typical image formation system as

$$E = L \frac{\pi}{4} \left(\frac{d}{h}\right)^2 \cos^4 \phi, \tag{2.8}$$

where h is the focal length of the imaging lens, d is the diameter of its aperture and ϕ is the angle subtended by the principal ray from the optical axis. In an ideal system, the brightness recorded is given by

$$I = Et \,, \tag{2.9}$$

where t is the time the image detector is exposed to the scene.

The radiometric response of ideal system is given by,

$$I = Lke, \tag{2.10}$$

where, $k = \cos^4\phi/h^2$ and $e = (\pi d^2/4)\, t$, e is the exposure of the image, which could be altered by varying either the aperture size d or the duration of exposure t.

Virtually any response function can be modeled using a higher- order polynomial, [Mitsunaga et al., 1999].

$$I = f(M) = \sum_{n=0}^{N} c_n M^n \,. \tag{2.11}$$

The self calibration algorithm considers two images of a scene taken using different exposures, e_q and e_{q+1} where the ratio is given by $R_{q,q+1} = e_q/e_{q+1}$.

The response function is recovered by formulating an error function which is a type of least squares solution

$$\varepsilon = \sum_{q=1}^{Q} \sum_{p=1}^{P} [\sum_{n=0}^{N} c_n M_{p,q}^n - R_{q,q+1} \sum_{n=0}^{N} c_n M_{p,q+1}^n]^2 \tag{2.12}$$

This method is not directly suitable for applications where the camera used does not have a varying lens.

The spectral and radiometric calibrations of thermal IR cameras are described from first principles in [Mermelstein et al., 2000]. The calibration setup uses a blackbody calibrator and the setup is shown in Figure 2.3.

The spectral response of the system is first obtained and then the radiometric calibration is done. The blackbody source with a surface emissivity is $\varepsilon_{BB}(\lambda)$ is maintained at a source temperature T_s. The assumption is that the blackbody source is a Lambertian emitter with a spectral radiance given by

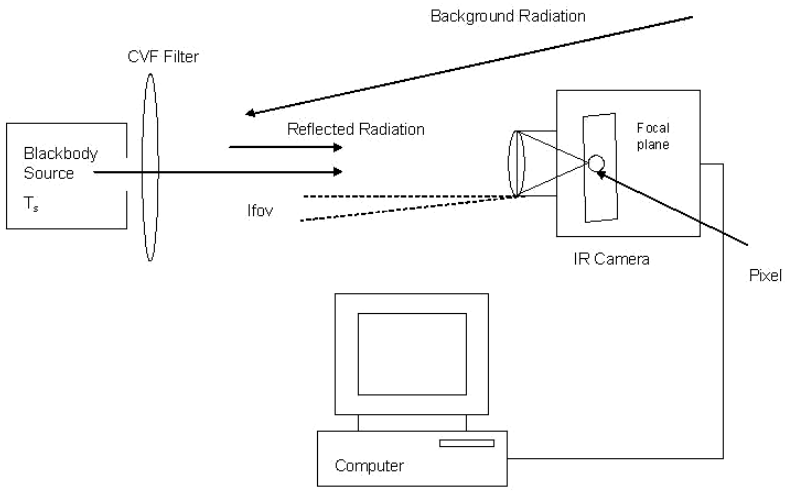

Figure 2-3: Setup for spectral calibration [Mermelstein et al., 2000].

$$L_\lambda(\lambda,T) = \varepsilon_{BB}(\lambda) M(\lambda,T)/\pi \tag{2.13}$$

where $M(\lambda,T)$ is the spectral radiant exitance of an idealized blackbody.

In spectral calibration, optical radiation emitted by the blackbody is passed through a continuous variable filter (CVF), which is an optical disk whose passband is adjusted by the disk rotation angle. The hot pixel and cold pixel digital counts are calculated and the camera spectral responsivity is calculated.

$$R(\lambda_0) = \frac{\Delta C(\lambda_0, T_s, T_o)}{G\alpha[P(\lambda_0, T_s) - P(\lambda_0, T_o)}} \tag{2.14}$$

The objective of the radiometric measurements is to measure the product of the detector responsivity α and gain G given the camera spectral response function $R(\lambda)$. The formula is given by [Mermelstein et al., 2000]. The exact radiance is measured at a number of temperature set points labeled by the index j and is given by

$$L_j = \int d\lambda.R(\lambda).\left\{[1-\rho_{BB}(\lambda)]\frac{M(\lambda,T_j)}{\pi} + \rho_{BB}(\lambda)\frac{M(\lambda,T_0)}{\pi}\right\} \tag{2.15}$$

where $\rho_{BB}(\lambda) = 1 - \varepsilon_{BB}(\lambda)$ is the reflectivity of the blackbody surface.

To obtain accurate temperature information, thermal imager requires calibration, which can be by reference to a blackbody source of known temperature or by spectral radiometric calibration, against calibrated reference detectors. Radiometric calibration of thermal imagers provides [Fox et al., 1995]:

1. Information to make it possible for an imager to make absolute temperature measurements in difficult environments or of surfaces with varying emissivity
2. Valuable additional information for the imager user or manufacturer to compliment a calibration from a blackbody.

The output signal from a thermal imager is the sum of the radiation emitted by the target, radiation emitted by the surroundings and reflected by the target, and radiation emitted by the atmosphere itself,

$$V(T) = k\{\int_0^\infty \varepsilon(\lambda)A(\lambda)P(\lambda,Tt)R(\lambda)d\lambda + \int_0^\infty [1-\varepsilon(\lambda)]A(\lambda)P(\lambda,Ts)R(\lambda)d\lambda + \int_0^\infty [1-A(\lambda)]P(\lambda,Ta)R(\lambda)d\lambda \tag{2.16}$$

where *V(T)* is the imager signal, *k* is the constant associated with the imager which is a function of the *f* number of the lens, *ε(λ)* is the target emissivity, *A(λ)* is the atmospheric absorption, *P(λ,T)*is the blackbody function, *R*(λ) is the spectral response of the camera (detector and optics), T_t, T_s, and T_a are the temperatures of the target, surroundings and the atmosphere respectively.

Parameters k and *R (λ)* are specific to the particular imaging system and are included in the algorithms for estimating the target temperature, *Tt,* after the user has given the values for surface emissivity ε and the surrounding temperature *Ts*.

An automated calibration system developed to calibrate IR flight cameras for series of sub-orbital experiments is presented in [Park et al., 1992]. The output of calibration is a set of calibration coefficients which convert the gray level output of the camera into physical units of radiance. The camera is placed in an environment chamber with preset ambient temperature settings that are changed and the blackbody temperatures are varied over the range where the camera's response is from its dark noise level to its saturation point. The collected data is sorted first and the calibration equation to convert the digital gray level to radiance is determined. The digital gray level and the radiance are related to

one another based on the calibration equation which varies depending on the detector used. A gray level fit is done based on the following equation [Park et al., 1992]

$$\begin{aligned} d &= C_1^p L\tau + C_2^p \tau + C_3^p + B_i + A_2\tau^2 + A_3\tau^3 \\ \sigma^{2=} &K_1^p L\tau + K_2^p \tau + K_3^p \end{aligned} \tag{2.17}$$

where d is the digitized gray level (0-255), σ^2 is the temporal variance of gray level for each pixel, τ is the integration time, L is the radiance , B_i is the gray level offset coefficient, A_2, A_3 is the integration time dependent analog background subtraction coefficients, C_1^p is the coefficient for sensitivity to incoming light level for each pixel, C_2^p is the coefficient for the noise rate of background collected by each pixel, C_3^p is the coefficient for the fixed pattern signal associated each with pixel.

Thermal infrared camera calibration technique using the wireless "smart" micro electro-mechanical (MEMS) sensors is discussed in [Bajcsy et al. 2004]. To obtain temperature profile information from a thermal IR image and to discriminate hazardous temperatures from harmless temperatures, it is necessary to convert the raw image values into engineering units, such as degree Celsius or Fahrenheit. The indoor experimental setup includes the thermal IR camera and the Modular Interactive Classification Analyzer (MICA) sensors providing temperature and luminance readings. Two calibration setups are developed one to calibrate the MICA temperature sensors and the second to calibrate the thermal IR camera as shown in Figures 2.4 and 2.5

Three main steps are carried out in the calibration of MICA sensors. The first step is to program the MICA sensors to sense and send temperature readings over a certain time period. During the same time period, the temperatures are also collected with a thermometer. A calibration transformation is established for MICA temperature sensors as a combination of factory recommended formula and thermometer measurements.

MICA sensors are programmed to sense and track time based on an incremental counter, and send counter state together with temperature readings after receiving a RESET signal. One increment of a counter corresponds to 100 ms. Both thermal IR camera and MICA sensors are initiated to acquire data by broadcasting a RESET signal to MICA sensors and triggering thermal IR camera acquisition. MICA sensors transmit every set (packet) of temperature measurements with the state of the internal counter to the base station attached to a personal computer (PC). Meantime, the thermal IR camera acquires data with the time stamp of the CPU clock counting from the RESET signal. The MICA raw temperature measurements are received and transformed into degrees Celsius. MICA temperature sensor locations in the thermal IR image are identified, and statistics of the transformed MICA temperature measurements and the thermal IR image pixel values at the MICA sensor locations are related to form the final calibration transformation.

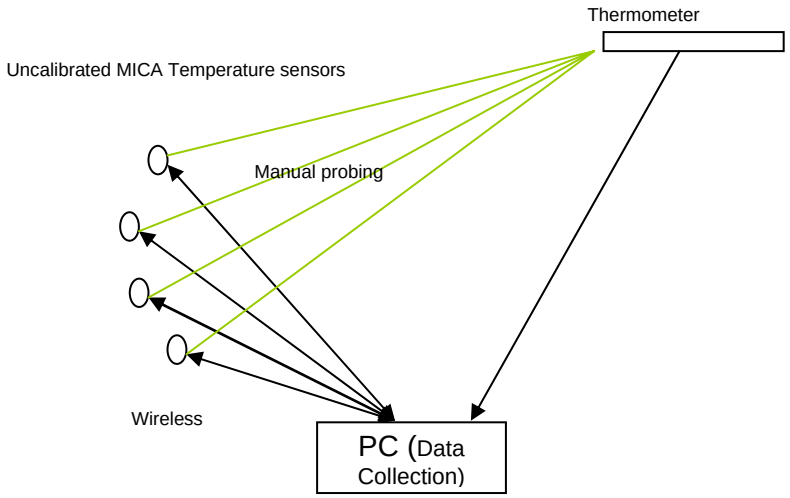

Figure 2-4: Setup for calibrating MICA temperature sensor measurements [Bajcsy et al.2004].

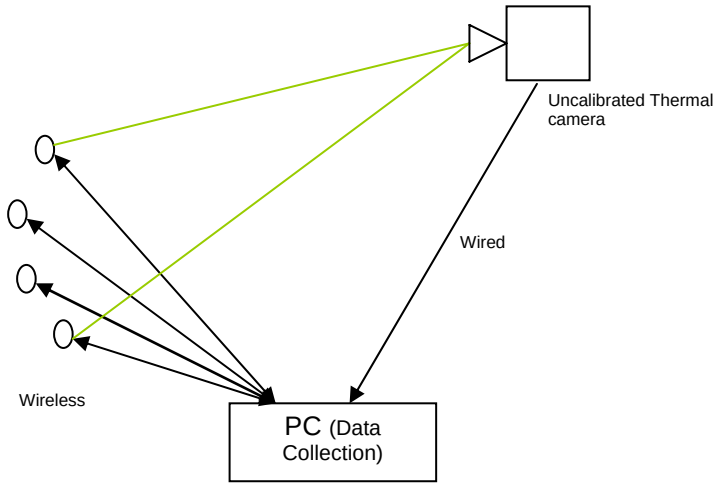

Figure 2-5: Setup for calibrating thermal IR camera measurements [Bajcsy et al.2004].

The parameters of importance for valid calibrated infrared signature are discussed in [Chevrette, 1986]:

i. The first and most important parameter is the exact spectral response $R(\lambda)$ of the thermal imager used. The spectral response determines the exact amount of radiation received from the reference source or the target.

ii. The signal transfer function is a curve that represents input/output relation of the camera and thus shows its dynamic range and its linearity. For example, the transfer function curve can be plotted between the video output voltage and the input target radiance for a fixed offset voltage

iii. Other data of importance is the table of the radiance gain ratios between the different gain settings for constant output signal voltage difference. The radiance gain ratio between gain setting G_1 and gain setting G_2 is defined by

$$RG_{12} = \frac{\Delta L_{G_1}}{\Delta L_{G_2}} = \left| \frac{\text{radiance variation on } G_1}{\text{radaince variation on G}_2} \right|_{\text{constant}\Delta V_s} \tag{2.18}$$

RG_{12} could also be defined as the ratio of the voltage differences on G_1 and G_2 for two reference blackbodies at fixed temperature, which is useful for calibration purposes.

iv. Other useful parameters are the modulation transfer function, which relates the image quality to its spatial frequency content. This gives an idea of the resolution capability of the imaging system.

Calibration Principle

Most of the calibration procedures reviewed so far use a blackbody source of known emissivity, and sometimes the assumption is that the emissivity is independent of wavelength and atmospheric absorption is zero. Hence, for the calibration setup, we need a blackbody calibrator whose temperature can be controlled and varied.

The components for calibration setup include:

i. IR system
ii. optical path between target and IR system
iii. target characteristics
iv. reference blackbodies

The apparent target irradiance E_{ap} is given by

$$E_{ap} = F(r)\int_{\lambda_0}\left[\{\varepsilon_t M(\lambda,T_t)+\rho_l M(\lambda,T_{ae})\}\tau_a(\lambda,r)+[1-\tau_a(\lambda,r)]M(\lambda,T_a)\right]d\lambda \tag{2.19}$$

If the target completely fills the IFOV, then *F(r)* is the system IFOV, Ω_s. The target radiance *L* is given by

$$L = \frac{E_{ap}}{F(r)} = \frac{E_{ap}}{\Omega_s} \tag{2.20}$$

In the absence of knowledge about the reflected background radiation $\rho_l\ M(\lambda,T_{ae})$ or if the target emissivity is unknown, the target area is taken as a blackbody and the radiance is given by

$$L = \int_{\lambda_0}\{\tau_a(\lambda,r)L(\lambda,T_{ap})+[1-\tau_a(\lambda,r)]L(\lambda,T_a)\}R(\lambda)d\lambda \tag{2.21}$$

where $\tau_a(\lambda,r)$ is the atmospheric transmissivity over the optical path between the imagers and the target, *r* is the range between the system to the target, $R(\lambda)$ is the system relative spectral response, T_{ap} is the apparent target temperature and T_a is the air temperature.

The detector voltage *V*, assumed to depend linearly on the radiance *L*, for a given gain setting is found from

$$V = gL + V_{off} \tag{2.22}$$

where *g* is the system responsivity and V_{off} is the DC offset

The gray scale *G(i)* (*i*= number of the gray level) is related to the detector output *V(i)* and apparent radiance *L(i)* by

$$\begin{aligned} L(i) &= aG(i) + L_{off} \\ G(i) &= \alpha V(i) + G_{off} \end{aligned} \tag{2.23}$$

where L_{off} is the radiance offset (constant), *a* is a constant, relating radiance to gray level, α is a constant, gray level to detector voltage and G_{off} is the gray level offset (constant)

For non-varying system parameters, the relations given in Eq2.23 are constant. In this case, the coefficients are determined by placing two blackbodies directly in front of the aperture, eliminating atmospheric attenuation.

The apparent radiance L_A and L_B for the two blackbodies (gray-levels G_A and G_B) located directly in front of the aperture and set at temperatures T_A and T_B is

$$L_A = \int_{\lambda_0} L(\lambda, T_A) R(\lambda) d\lambda = aG_A + L_{off}$$
$$L_B = \int_{\lambda_0} L(\lambda, T_B) R(\lambda) d\lambda = aG_B + L_{off} \quad (2.24)$$

Calibration parameters

The spectral response $R(\lambda)$ is a specific system constant and must be measured and determined in the laboratory. Under normal conditions the spectral response does not change with time. Two more experimental parameters required are the air temperature T_a and the spectral atmospheric transmissivity $\tau_a(\lambda,r)$.Two blackbodies are necessary to solve for the calibration coefficients in Eq2.23 [Jacobs,1996]. The blackbodies are placed at approximately the same bearing and range r as that of the target as shown in Figure 2.6.

The steps to be followed for calibration are as follows:

1. Select system gain to produce an image without saturation

2. In the first step, the aperture apparent radiance L_A and L_B for the two blackbodies, set at temperatures T_A and T_B are calculated from

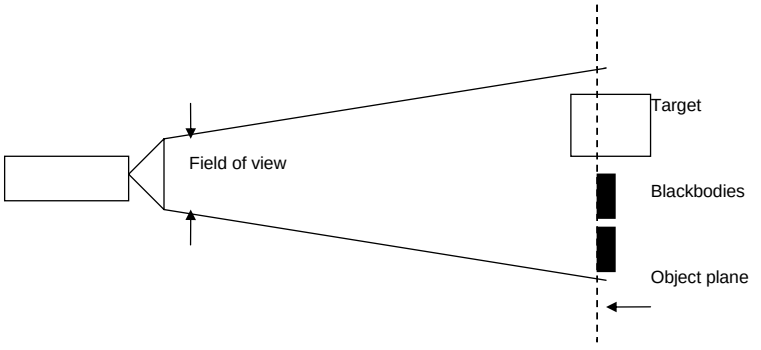

Figure 2-6: Blackbodies and the target at the same range [Jacobs, 1996].

$$L_A = \int_{\lambda_0} \{\tau_a(\lambda,r)L(\lambda,T_A) + [1-\tau_a(\lambda,r)]L(\lambda,T_a)\}R(\lambda)d\lambda$$
$$L_B = \int_{\lambda_0} \{\tau_a(\lambda,r)L(\lambda,T_B) + [1-\tau_a(\lambda,r)]L(\lambda,T_a)\}R(\lambda)d\lambda \quad (2.25)$$

3. Next, determine the relation between radiance and gray-level by calculating the coefficients a and L_{off} using the gray-levels of the blackbodies, G_A and G_B, from

$$L_A = aG_A + L_{off}$$
$$L_B = aG_B + L_{off} \quad (2.26)$$

A gray-level on the target G_t can now be converted to a corresponding radiance value. The apparent target temperature T_t is found from L_t, where $L_t = a\ G_t + L_{off}$, by inversely solving the integral given by Eq2.20 to obtain L as

$$L_t = \int_{\lambda_0} \{\tau_a(\lambda,r)L(\lambda,T_t) + [1-\tau_a(\lambda,r)]L(\lambda,T_a)\}R(\lambda)d\lambda \Rightarrow T_t \quad (2.27)$$

2.4 Temperature Data Measurement using IR Thermometer

Temperature plays an important role in the automotive industry which indicates the condition of the product, both in manufacturing or in quality control. Accurate temperature monitoring of automotive components aids in improving the quality of the component and also aids in simulating the prototype and testing of the automotive part in the virtual environment. Radiometric methods are used when contact with the heated object is undesirable or impossible. These conditions occur, for example, when the target is in motion, in rotation, or in vibration or under go rapid thermal changes or when the target temperature is high, as in the case of automotive parts where the intense heat would degrade or destroy the contact temperature sensor.

Non-contact thermometers provide superior response time, durability, non-contamination and ease of use [Dewitt et al., 1988]. Though infrared (IR) thermometers are easy to use, there are certain conditions to be met while using them. The optics of the sensor must be protected from dust and condensing liquids, and the target must be infrared optically visible to the infrared thermometer. High level of dust and smoke make measurements less accurate. The infrared thermometer measures surface temperatures and not the inside temperature values of the automotive component.

The basic design principle of an infrared thermometer shown in Figure 2.7 includes the target, the transmission medium, infrared filter or optics, detectors and the display and interface. When the temperature is measured by a noncontact device, the IR energy

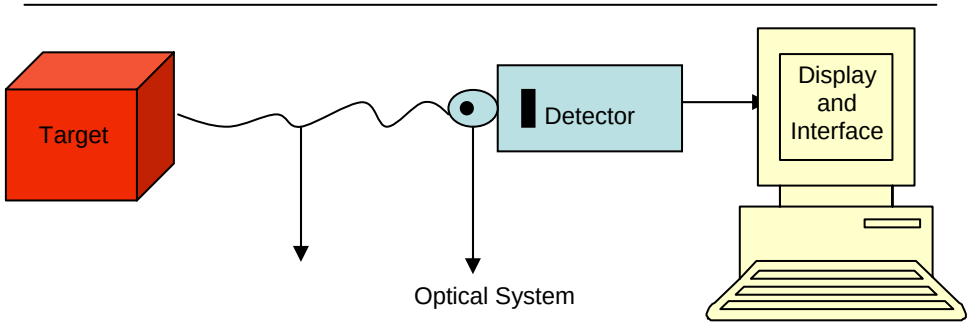

Figure 2-7: Basic components of an infrared thermometer.

emitted from the target passes through the optical system of the thermometer and is converted to an electrical signal at the detector. This signal is then displayed as a temperature reading.

The Target

Objects that are above absolute zero emit infrared radiation according to its temperature, which is normally invisible to the naked eye. The internal mechanical movement of the molecules results in emission of electromagnetic radiation. The radiation can be reflected, absorbed and/or transmitted. The target temperature range, size and material influence the selection of appropriate temperature measurement instrument. The emissivity of the target is an important factor to be considered when measuring surface temperatures. The target could be a metal or a non-metal, could be shiny or polished, hence the emissivity value of the target varies based on the material and is different for different wavelengths. Adjustable emissivity setting aids in changing the emissivity based on the target surface. If the target to be measured is glass, then both reflectance and transmittance must be considered.

Ambient Conditions

The transmission medium, in the path of the infrared thermometer (usually the ambient air) affects the temperature measurement of the target. Components such as vapor and carbon dioxide in the atmosphere absorb infrared radiation at particular wavelengths which may result in transmission loss. In order to overcome such problems, manufacturers provide certain infrared spectral bands which do not contain these

absorption bands. The most commonly used is 8-14μm. The thermal radiation of the target surroundings should also be taken into account. Dust or smoke in the atmosphere results in contamination of the optics and therefore, in false temperature measurement. Proper measures should be taken to avoid such situations. Infrared thermometers are also subject to operating temperatures which, when exceeded, may result in improper temperature measurement.

The Optical system

The optical system of the infrared thermometer detects the emitted infrared energy emitted from a circular measurement spot and focuses it on a detector. The target must completely fill the field of view to avoid other background temperature interference. The optical resolution is defined as the relationship between the distance of the measuring device from the target, and the diameter of the spot (D:S). The greater this value, the better the resolution of the measuring device, and the smaller the spot size that can be measured. The laser beam included in the system aids in aiming at the measurement spot for moving objects and or in poor light conditions.

Detectors

The detector is the most important component in the infrared thermometer. It converts the infrared radiation received from the optical system into an electrical signal, which is displayed as temperature values. There are two types of infrared detectors in use, namely quantum detectors and thermal detectors. Quantum detectors directly interact with the photons emitted to produce an electrical signal whereas thermal detectors change their temperature depending upon the impacting radiation.

The Display and Interface

The electrical signal from the detector is displayed as temperature values in the display monitor. Hand-held thermometers have a directly accessible display and control panel combination which acts as the primary output of the measuring device. Other secondary output devices like printers, data loggers or PC can also be attached to the IR thermometers in use. Such devices provide remote control of the IR thermometer and also aids in changing emissivity settings easily.

There are several important factors that determine accurate temperature measurement. The most important among them are the emissivity, distance to spot ratio and the field of view.

Emissivity is the measure of an object's ability to emit infrared energy. Emitted energy indicates the temperature of the object. Emissivity can have a value from 0 (shiny mirror) to 1.0 (blackbody). Most organic, painted, or oxidized surfaces have emissivity values close to 0.95. Infrared thermometers have options for adjustable emissivity or some have

fixed emissivity. Since emissivity varies from surface to surface and between wavelengths it is always important to measure the emissivity of the surface or find out the material and set the emissivity based on the emissivity tables provided by the manufacturers.

Distance to spot ratio is the ratio of the distance from the instrument to the target compared to the size of the measurement spot. As discussed earlier, the higher the ratio is, the better the instrument's resolution and smaller the spot size.

The target size should be greater than the field of view or the spot size of the unit used for measuring surface temperature. For better accuracy, the target should at least be twice as large as the spot size. This aids in avoiding the unwanted background temperatures.

3 SIMULATION OF SYNTHETIC THERMAL IMAGES

Thermal problems in mechanical and electronic systems are often difficult to detect and resolve because of the complex effects of convection or radiation. This chapter describes briefly the need for simulation of thermal images in the virtual environment and gives an intuition into the state of the art of simulating thermal images and the requirements for such simulation including the software used for simulation. Section 3.1 gives a brief introduction to the need for simulation of synthetic thermal images and the applications and the necessary use of it in the automobile industry. The basic requirement for simulation and the definition of properties are discussed in Section 3.2. Finally Section 3.3 discusses the software used for simulation of synthetic thermal images.

3.1 Need for Thermal Image Simulation

In recent years, in order to reduce the vehicle development time by one third, most of the automotive companies are considering ways of improving the test process and reducing the number of design iterations and it is necessary to analyze the thermal heat distribution occurring in automotive parts in order to make those components robust under any thermal conditions. Computational fluid flow analyses in thermal simulation software allow engineers and designers to digitally test a virtual vehicle without building a physical prototype.

Infrared imaging methods provide unequaled ease and flexibility for investigating any object temperatures that are under consideration. Infrared measurements are not only accurate but also they are fast and offer the least disturbance to the point being measured. Thermal images are unique for every object based on the infrared radiation emitted by the object. The object, which is not able to radiate energy in the visible spectrum, radiates in the infrared band. Thermal imagers are used to detect the infrared radiation and convert them to the visual band to visually see the images. Thermal imagers are the detector and lens combination, which detects the infrared radiation and converts the radiation to the visual band.

Effectiveness of thermal cameras depends on their operators. The three possible cases which results in poor results are:

- The spectral range of the thermal cameras differs from the spectral range of human eyes, and so the thermal image differs from the visual image of the same scenario

- The thermal cameras are not stereoscopic systems like human eyes and it is difficult to estimate the range to different objects seen in the thermal image

- There are no shadows in the thermal images which provide human information about the source of illumination of the scene

Development of prototype and testing environments can be avoided for each and every testing by simulating the real time components and some of the reasons that hold strong for the simulation are described below:

- Simulation of under hood/ under vehicle components helps to identify and resolve the vehicle thermal issues early in the design phase

- Simulation of automotive components in virtual environments helps military vehicles to get into camouflage and also to identify target camouflages

- Simulation aids in inspection and predictive maintenance, where a database of simulated images can be used for comparison of various circumstances

- Simulating real-life conditions digitally can considerably reduce the time and expense of building physical prototypes to test every variation

Virtual simulations are becoming a necessary process also in every field with deals with thermal management. Even in the medical field, such simulations play a vital role in modeling the effects or counter effects of a particular vaccine in the human body. The automotive industry and the military services rely more on simulation to model the thermal heat flow in the vehicle in order to overcome the thermal load on components surrounding high temperature sources and to camouflage. Simulation of under hood/ under vehicle components poses several challenges and many requirements which are discussed in the next section.

3.2 Fundamentals of Thermal Modeling

Image synthesis involves the knowledge and understanding of the governing parameters and equations. Simulation of thermal images is achieved based on the thermal radiation properties of the object under consideration. A general introduction to thermal imaging and black bodies was given in Chapter 2. This section discusses the equations that result

in the simulation of thermal images. The net heat exchange due to radiation between two arbitrary surfaces that are not blackbodies can be described as in [Lienhard et al., 2004],

$$Q_{net} = A_1 F_{1-2} \sigma (T_1^4 - T_2^4) \tag{3-1}$$

where T_1 and T_2 are the surface temperatures of the two surfaces, F_{1-2} is the fraction of energy that is emitted from surface 1 and absorbed at surface 2 both directly and by reflection, A is area, and σ is the Stefan-Boltzmann constant.

The radiation phenomenon is a nonlinear process because the thermal energy emitted due to radiation is proportional to the fourth power of absolute temperature. It is shown by Ketkar [Ketkar, 1999] that to compute the radiation heat transfer between two surfaces, it is necessary to introduce the concept of radiation view factor or configuration factor or shape factor. A viewfactor, F_{ij}, is defined as the fraction of thermal energy that leaves the surface i and is incident on the surface j. The view factor can be defined as

$$F_{ij} = \frac{1}{A_i} \int_{A_i} \int_{A_j} \frac{\cos\theta_i \cos\theta_j}{\pi R^2} dA_i dA_j \tag{3-2}$$

where A_i and A_j are the areas of the surfaces i and j respectively, θ_i and θ_j are the angles between the position-dependent normal vectors to surfaces i and j and a line of length R connecting the points of evaluation of the normals.

Similarly for F_{ji}, it can be modeled as Eq3-2 and hence it follows that

$$A_i F_{ij} = A_j F_{ji} \tag{3-3}$$

The above equation is known as the reciprocity relation of viewfactors. This relation is used to compute viewfactors from the other known viewfactors and reduces the number of viewfactors to be calculated.

The basic assumptions used in deriving Eq.3-2 are:

a) The two surfaces are diffusively emitting and reflecting.
b) The two surfaces are isothermal.

For an enclosure of N surfaces, the

$$\sum_{j=1}^{N} F = 1_{ij} \tag{3-4}$$

For a linear system, the radiosity solution produces finite number of viewfactor equations that must be solved. The computation of viewfactors is a complex task and can be done in

different ways. The different methods for viewfactor calculation and the solutions for resulting viewfactor equations are discussed by Kaksonen, [Kaksonen, 2002]. The calculation of viewfactors is a time consuming task and it increases the time of simulation for highly voluminous mesh. The integral given in Eq3.2 can be solved to obtain the viewfactors analytically. Other methods that can be used are the differential area sampling or area to area sampling methods.

MuSES uses the hemi-cube method to calculate the view factors, described in [Curran et al., 1995]. The basic algorithm begins by discretizing the surface of the hemicube into a set of M uniform subpatches which will be called pixels. Each pixel defines a particular direction and angle from the receiving patch's centroid. Thus each pixel contributes a specific delta-view factor value to the overall view factor between two surfaces if the pixel is covered by the projection of the transmitting surface onto the discretized hemicube. Each pixel in the rendered image is assigned a weight such that summing up the weights for all the pixels corresponding to the same thermal node yields the view factor from the thermal node at the viewing point to the thermal node scanned in the image. MuSES assumes that the geometry has been previously meshed for finite element use by choosing the centroid of each element as the points at which view factors are computed.

3.3 Requirements for Simulation

The simulation of thermal images in the virtual environment needs to incorporate the conditions and the thermal properties of the real time system in order to obtain better results. The knowledge of the simulation type and the identification of perfect component for analysis, the material and thermal properties and the use of perfect geometry are required prior to simulation. The knowledge of these properties helps in obtaining a better thermal signature prediction of the component under consideration and also helps in fine tuning of the simulation environment for better results. This subsection discusses the basic knowledge that is required prior to thermal signature modeling.

Geometry of Components

Geometry of the model under consideration is the most important requirement for thermal modeling. Geometry is most often composed of vertices, curves, surfaces and solids as described by a CAD or solids modeling package. The geometry of the component under study should be in a form acceptable by the simulation software used. The geometry normally used is a surface description of the component used for thermal modeling. The proper meshing of the geometry is discussed later in this section. The mesh could be from CAD or from other 3D modeling tools or could also be generated by reverse engineering the model by laser scanning and reconstructing the model from the scans. The complete under vehicle chassis shown in Figure 3.1 is represented as CAD mesh in Figure 3.2.

Figure 3-1: Visual image of the Toyota Tundra under vehicle chassis**.**

.

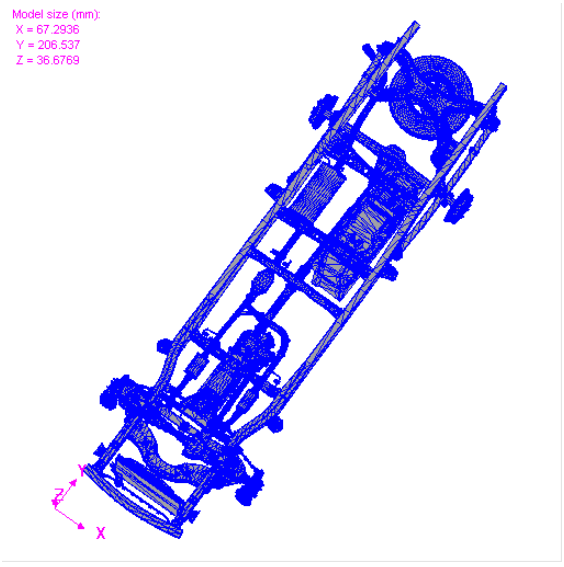

Figure 3-2: Surface mesh of the Toyota Tundra under vehicle chassis.

The outer body surface and inner components surface mesh is created using the commercial meshing software or created using CAD. The CAD mesh often contains holes and needs to be cleaned up before using it for thermal simulation of under hood/under vehicle components. All the components have to be meshed properly in order to obtain better thermal flow analysis. The process of meshing and the requirements for good meshing are discussed in the next few paragraphs

The CAD models are normally voluminous [Srinivasan et al., 2004] or complex and hence reduction of the mesh size is a necessary step. The engine compartment consists of 100 components and the CAD meshes represent each and every component as a single assembly and hence the size of the model is huge. The simulation time required is affected by the size of the model and the number of elements in the model. CAD models are not readily available from the manufacturers with all the details of the interiors. This necessitates the generation of 3D model meshes from other sources. As-built automotive components can be modeled as they are using the concept of reverse engineering, which in simple terms can be defined as the generation of 3D meshes by laser scanning the model and reconstruction from that scan. The automotive parts are scanned with the help of a range scanner and the multiple views are registered to form a single view, which is then triangulated to form the 3D model [Page et al., 2003].

Meshing Requirements

Meshing can be defined as the process of breaking up a physical domain into smaller sub-domains (elements) in order to facilitate the numerical solution of a partial differential equation. Meshing can be used for a variety of applications. Finite element meshing is the basis for most of the applications. Surface domains are normally subdivided into triangle or quadrilateral shapes, whereas volumes are subdivided primarily into tetrahedral or hexahedral shapes. Automatic meshing algorithms ideally define the shape and distribution of the elements. The automatic mesh generation problem attempts to define a set of nodes and elements in order to best describe a geometric domain, subject to various element size and shape criteria.

The process of creating a thermal mesh is a complicated task, which requires modeling expertise and advanced tools [MuSES]. The process of generating meshes is not a linear process. Mesh generation starts with an existing geometry and produces a quality thermal model depending on:

i. Geometry type (mesh or CAD source)
ii. The modeler's preferences
iii. The condition of the source geometry
iv. Special thermal modeling techniques

v. The desired final model resolution

For thermal signature modeling, the 3D mesh of the component under consideration should be complete without any holes or missing elements. The meshing should also have uniform aspect ratio and uniform normal; this avoids the directional effects of heat flow and makes it easier to concentrate on one direction or in the direction we assume. The meshes could be CAD meshes or polygonal meshes from NURBS surfaces or LASER scanned and reconstructed meshes. The mesh used for simulation should be finite and should have a medium complexity. Voluminous meshes not only increase the size of the model also increase the numerical solution computing time and the time used for actual simulation. In such cases, the thermal solution is not obtained for each and every element which further increases the time for simulation.

Mesher – It is the tool which is used to generate meshes for the given geometry. Filling the surface creates the mesh. The common factors in the meshing process are:

i. Import the mesh or CAD data into the mesher
ii. Clean up the geometry so that edges and vertices line up (heal, repair, or create geometry)
iii. Identify the hard (large angle feature) edges
iv. Mesh using an algorithm that preserves the geometry as best possible while minimizing the element count and maintaining element quality.

Idea of Simulation

Thermal images have a wide variety of applications and they are nothing but the representation of the heat radiated by the component under consideration. The simulation idea should be clear before we simulate the thermal image of any particular component. A thermal model can be created for analyzing the heat distribution in the component over a period of time, it could be created for inspection of any abnormalities in the scene or it could be for evaluation of thermal signature for different vehicle components. For different types of simulation it is necessary to incorporate the required parameter for that type of simulation. For example with the analysis for different vehicles it is necessary to know about the different vehicles temperature curve and other material surface properties.

Identification of Components

The component selected for thermal modeling should show some temperature variations with respect to time. If the component undergoes a very minute change in temperature, the modeling time will be very small (i.e. nanoseconds) which might be very difficult to view in the simulation software. The exhaust system (Figure 3.3 (a) and (b)) is the best system for thermal modeling because the system shows significant changes in temperature with respect to time.

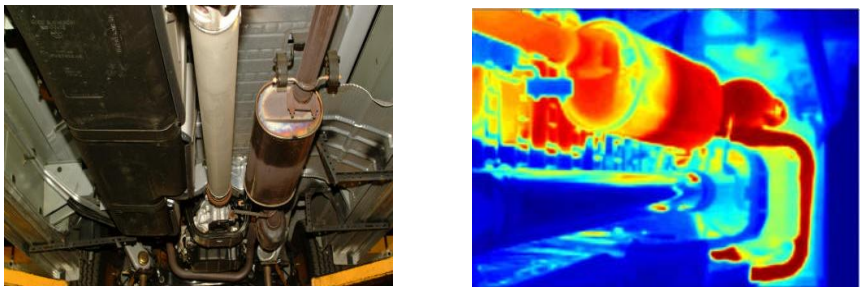

(a) (b)

Figure 3-3: (a) Visual image of the exhaust system components and (b) Thermal image of the exhaust system components showing temperature variation red is hot and blue is cold.

Parameters for thermal modeling

In the simulation of under hood and under vehicle automotive components, the thermal modeling necessitates the knowledge of certain parameters like the environmental conditions surrounding the vehicle, temperature curves of the components with respect to time and the materials of the component surfaces and their emissivities. This sub section discusses in detail these parameters, assignment of properties is also discussed in this section.

Environmental conditions – The environmental parameters like the wind direction, humidity, solar irradiance and the cloud cover determine the starting ambience of the vehicle. These parameters initiate the necessary heating up of the engine components when the vehicle is first started. If the surrounding atmospheric temperature is very low, then the engine takes up a lot of time for initial heating. Hence it is necessary to know the environmental conditions. This also aids in simulating thermal images of under hood/ under vehicle components for a particular day or for a particular period of time, which in turn aids in inspection. For example, such type of inspection may be necessary for inspecting a car parked in a parking lot for a long time.

Temperature curves – Simulations of under hood/under vehicle components have not received much recognition though they have been in use for several years [Damodaran et al., 2000]. This lack of recognition is mainly due to the non capability of providing actual temperature variations with respect to time for the component under study. Exact prediction of temperature variations would be an important improvement to the model. In

order to achieve this, improvement steps for measuring the temperature variations are to be done. The solution for this problem is to measure the temperature variations with the help of an infrared thermometer, which works similar to an infrared imaging device, and displays the temperature values with respect to time. These temperature curves can be incorporated into the simulation algorithm for better improved results.

Engine: The inside temperature of the engine is very high because of the combustion taking place within the engine. In real time, coolant fluid flows through the engine block and carries away most of the heat and hence the outside temperature of the engine block is relatively less compared to the inside temperature. All these conditions are taken into account and the temperature curves are assigned. The temperature curve shown here is based on certain assumptions, such as the effect of fluid.

Muffler: The outer surface of the exhaust system is the primary source of heat in to the engine component. The surface temperature of the exhaust system components such as the manifolds, connecting pipes, catalytic converter, muffler etc., varies between 785K and 925 K, when the engine is operating at its maximum capacity [Srinivasan et al., 2004]. There is no flow of coolant fluid in real time, but however there occurs heat loss due to conduction, radiation and convection. This slightly reduces the outside temperature. The assignment of temperature curves to two parts, namely the engine and the muffler, is shown in Figure 3.4 and 3.5. These parts are selected here because the temperature curves vary widely.

The temperature curves are just predictions or assumptions based on the theoretical knowledge of the operation of the vehicle. As mentioned earlier, such assumptions can be avoided by measuring the real time temperature curve of the vehicle with respect to time and incorporating it in to the simulation process.

The measurement of temperature involves several challenges and also limitations. The infrared thermometer measures only the surface temperature and it does not provide any information on the inside temperature changes. The measurement process itself should be clear because the temperature measurement of various components cannot be achieved easily when the vehicle is in motion.

In order to overcome such challenges the temperature should be measured for each and every individual part by running the car at idle and taking measurements with respect to time. The engine compartment is a vast system with more than one hundred major components including the power-train, suspension, electrical, exhaust components etc.

Measuring the temperature curves for all the under vehicle automotive components is not an easy job and hence the temperature curves for some of the components, such as transmission, are assumed, whereas for the components, such as muffler, they are measured.

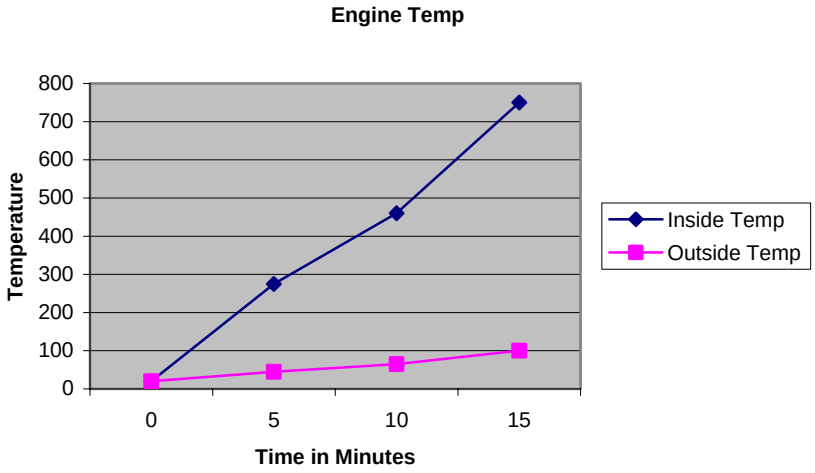

Figure 3-4: Engine temperature curve.

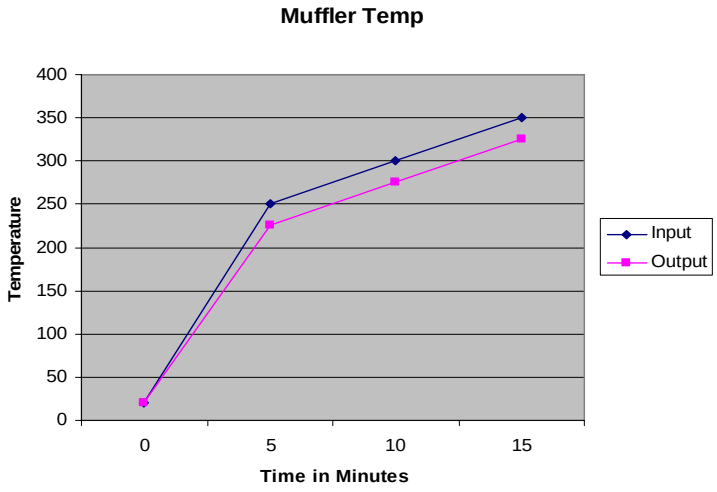

Figure 3-5: Muffler temperature curve.

Definition of Properties – The assignment of properties for the parts plays an important role in the thermal modeling of the components. The properties are assigned taking into account the real time situations and assumed to be very close to the real time values.

The various parameters needed for the model building are discussed below along with their importance and role in the thermal infrared prediction. The parameters assigned are:

1. Type of Material

   This parameter is assigned for calculated thermal parts only. Here based on the type of the material assigned, the numerical solution calculates the net energy incident on the element or part. The emissivity of the surface material plays an important role in the radiation of heat. The knowledge of the material used for making the components gives the thermal conductivity and the emissivity of the material, which in turn results in improved simulation.

2. Thickness

   The thickness value is used to determine the capacitance of the part and it is mainly used for conduction. It has no effect on the geometry used.

3. Surface condition

   The surface properties and paint code values are used to apply a surface emissivity value to the thermal calculations carried out. This is used to know how much heat is reflected from the part and how much is absorbed and emitted by the part.

   Paint code: The paint codes are specified for simulating the thermal image

   as seen through a sensor.

Effect of fluids – The systems in the engine compartment are forced to be at an acceptable temperature with the help of fluid flow. In general, the fluid flow in a heat engine is caused by [MuSES] active pressure sources that produce forced flow and passive pressure sources that produce natural flow. The heat flow in and out of the system is mainly coupled with the fluid flow.
The convective heat transfer coefficient (h), defines the heat transfer due to convection. It represents the thermal resistance of relatively stagnant layer of fluid between a heat transfer surface and the fluid medium.

The fluid flow effects can be modeled in a simulation or sometimes they are assumed to be virtually present by carefully designing the temperature curves such that the effects of fluid flow and the heat conduction or convection are also modeled.

Assignment of parts – The elements in a mesh of an automotive component are grouped into parts and similar parts are combined to form a complete under vehicle chassis. The parts have to be assigned the parameters discussed earlier. All the parts in the vehicle are not heated up by themselves and most of the components are heated up either by the process of conduction or convection or radiation. Hence parts with significant temperature changes are assigned temperature curves where as the other parts are assigned as calculated parts. The two type of parts are discussed in brief below

Assigned temperature parts

This part represents a group of elements that are assigned the same temperature. The temperature remains constant over time or varies with time. These parts can be connected to fluid parts through convection. They are the main heat source components like the exhaust system components or injector vessels in the engine where the temperature is very hot.

Calculated temperature parts

The calculated temperature parts represent groups of elements whose temperature variation are calculated through the numerical solution. The main parameter is the emissivity of the material used which aids in calculation of the temperature values of the component with respect to time. These parts are further divided as 1-layer, 2-layer or 3-layer parts.

Bidirectional Reflectance Distribution Function (BRDF)

In computer simulation of realistic images, it is necessary to know the description of reflectance for each reflective surface in the scene. The BRDF represents the ratio of radiance per unit irradiance, used for describing the geometrical reflectance properties of the surface. The BRDF depends on wavelength and is determined by the structural and optical properties of the surface, such as shadow-casting, multiple scattering, mutual shadowing, transmission, reflection, absorption and emission by surface elements, facet orientation distribution and facet density. The bidirectional reflectance distribution function as first presented by Nicodemus and described by Zissis [Zissis, 1975] is given by

$$f_r(\theta_i,\phi_i;\theta_r,\phi_r) = \frac{dL_r(\theta_r,\phi_r)}{L_i(\theta_i,\phi_i)d\Omega_i} \tag{3-5}$$

where θ_i and θ_r are the incident and reflected flux in one direction, Φ_i and Φ_r are the incident and reflected flux in other direction and Ω is the projected angle.

In the simulation sense, this function allows viewing the thermal results as seen through a sensor. The BRDF image uses the radiosity solution, environmental conditions and the viewing geometry. A two-step process is carried out to generate the BRDF image. In the

first step, radiance is computed for the centroid of the elements facing the sensor's position. This is carried out for all elements even if they are not surface elements.

Elements are mostly treated as two dimensional with a front and back surface. The pixels occupied by an undefined surface are considered to be 'bad pixels' and are excluded from the image statistics.

The second step consists of tracing a ray from the sensor position through the center of each pixel of the image. For each ray that intersects the model, its associated pixel is assigned the radiance of the element centroid closest to the sensor position. All pixels associated with rays that miss the target have the background radiance assigned to them.

3.4 Simulation of Thermal Images using MuSES

There has been increasing interest in and emphasis on the use of computer based analytical simulation of thermal phenomena in electronic and mechanical systems. With the knowledge from the parameters of Section 3.3, the simulation of the thermal images of automotive components is achieved using the software designed for thermal signature prediction. The MuSES (Multi-Service Electro Optic Signature) interface is optimized for engineers who need to incorporate signature management treatments or heat management solutions into vehicle design. MuSES thermal simulation software is a comprehensive heat transfer simulation package, which provides fast and accurate solutions to complex thermal problems [Johnson et al., 1998] and [Johnson et al., 1999]. MuSES can be used to model the steady state and transient heat processes including 3D-conduction, radiation and convection of heat over complex surface descriptions of component systems.

In simple words, MuSES predicts the thermal signature with a finite element surface description (mesh), groups the elements in the mesh in to parts which have the same material and surface properties. The view factors are calculated using numerical methods and the transient nodal temperatures are calculated and displayed using an implicit solution to the finite difference equations derived from the thermal properties of each node and the radiation exchange between nodes. Final result of the infrared prediction software is a temperature map of the component system, depicting the steady state and transient heat distribution.
MuSES' menu-driven GUI (see Figure 3.6) integrates the steps involved in building a signature model into a single, comprehensive modeling tool. Besides eliminating the need to step through various pre- and post-processing utilities, MuSES monitors the status of the model to insure that important steps are not skipped.

MuSES Graphical User Interface – MuSES interface screen has three major areas. The creation, model editing, results simulation and the analysis of results are done in these three regions.

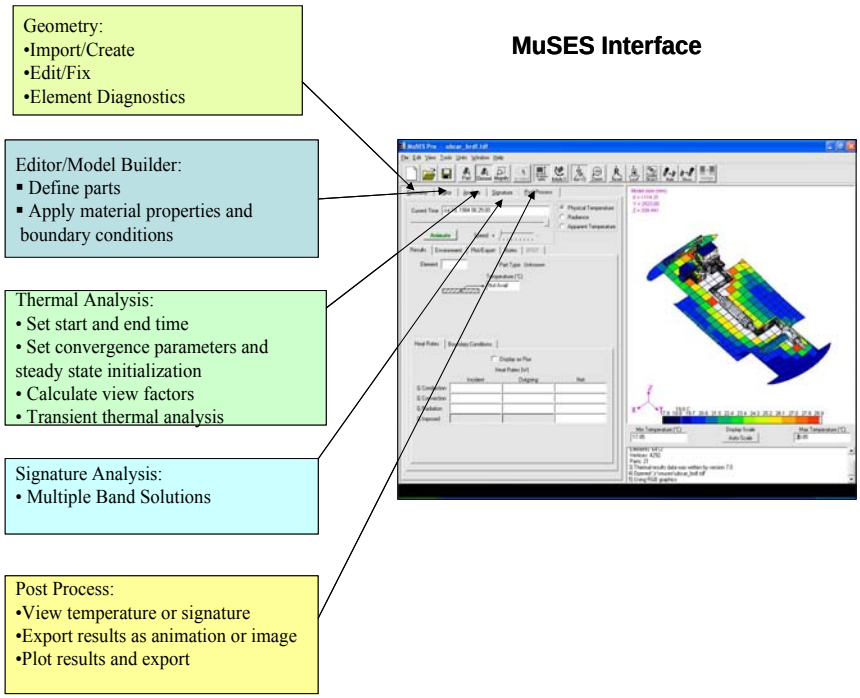

Figure 3-6: MuSES GUI interface detailing all the sub tabs.

1. **The selection window –** This window allows to perform operations like creating and editing, building the thermal model, analyzing the results, running signature simulation and to view the results of simulation. The selection provides five sub tabs, shown in Figure 3.6, for the various operations performed for the simulation of thermal images.

2. **Graphics window** – This is where the model geometry and the results of simulation are viewed. The elements are selected in the graphics window and can be grouped in to parts of same surface properties.

3. **Status window** –The status window keeps the commands executed while the modeling process is done. The number of parts, elements and the vertices in a given model are displayed in this window when the model is first opened.

MuSES Model Building

Simulation of under hood and under vehicle components requires the use of proper geometrical model representing the component under consideration. The CAD mesh is cleaned up and then imported into MuSES for simulation. Next the analysis of the solution occurs and here some more parameters that influence the final thermal simulation and the time required for the calculation of the thermal solution are discussed.

1. Start time, end time and step size

   The solution start time and end time are determined by the temperature curve assigned or by the user's requirements. If a weather file is used, the file containing all the environmental details for a particular day or for a particular period of time is included for analysis, then the solution start and end times are set automatically according to the weather data file. The step size is used in calculating the results. For example, if the step size is 1, then the results of the simulation can be seen for increments of 1 minute.

2. Tolerance and Tolerance slope

   Tolerance refers to the maximum nodal temperature change that occurred for any element between the current and previous iteration. The tolerance slope is the rate at which the tolerance (change in temperature) is changing. There occurs a trade off between the tolerance slope and the time taken for the thermal simulation. When the tolerance slope is very small, a large number of iterations are used to achieve the exact solution. If there is a restriction with the time taken for the simulation of the thermal image, then the tolerance slope can be relaxed to obtain the solution in a shorter time.

3. View factor rays

   View factor rays represent the number of rays that are cast from each element subdivision which will be used for calculating radiation. The solution time taken for accurate results will be more. Depending on the complexity of the model the solution time varies for the calculation of the view factor rays.

The MuSES solution procedure involves the following steps after the proper assignment of various parameters that are discussed earlier in this section.

- Group geometry – In MuSES, parts are groups of mesh elements which share the same
  - Boundary conditions

  - Material, physical and surface properties
  - Thermal properties

- Assign material properties – The thermal properties like material surfaces, temperature curves, thickness, surface emissivities are assigned

- Set boundary conditions – Once all the elements of a mesh have been assigned to specific parts, boundary conditions can be applied to them. Boundary conditions, as defined here, include environmental (weather and background) interaction, applied convection and/or applied temperature or heat assignments.

- Set solution parameters – The convergence parameters and the start and end time are assigned.

- Run simulation and signature simulation (optional) – Multiple band solutions can be solved for a particular component.

- View results using post-processor – The results are analyzed and further interpretations are done if necessary. The results can also be exported for future analysis.

4 EXPERIMENTAL RESULTS -THERMAL DATA ACQUISITION

This chapter presents the experimental results for real time thermal data capturing. The chapter begins with results of real time thermal image capture under normal conditions in Section 4.1. Temperature measurement results are described in Section 4.2. Section 4.3 describes the application of thermal image processing in the field of threat detection.

4.1 Thermal Images to Aid in Simulation

Real time thermal images of automotive components represent the heat pattern obtained as a result of conduction, convection and/or radiation. This section describes in detail the acquisition process of real thermal images of under vehicle automotive parts under normal working conditions for different vehicles. The objective of acquisition is to obtain a complete thermal sequence with respect to time spanning the entire under vehicle chassis of the vehicles to observe and analyze the heat distribution pattern of the automotive components. In order to achieve this objective, the under vehicle chassis was divided into sections, so that the complete chassis can be viewed. The Dodge RAM 3500 van and the Ford Taurus were used for data acquisition.

The Dodge RAM 3500 van under vehicle chassis was divided into three sections whereas the Ford Taurus chassis was divided into two sections. The first section of the van included the catalytic converter and the muffler of the vehicle used for image acquisition, the second section included the muffler, drive shaft and the axial and the third section consisted of the axial and the tail pipe of the muffler. The Ford Taurus's first section included the exhaust manifold pipes and catalytic converter and the second section included the muffler. The sequences of thermal images obtained were used as a basis for thermal modeling of the automotive components.

The vehicles used for image acquisition are shown in Figure 4.1 (a) and (b). Thermal data capture necessitates the running of the engine to take temperature variations with respect to time. For collecting a database of thermal images, the vehicle was jacked up and left running for the entire time of data capture. As explained in Chapter 2, Section 2.2, thermal imaging systems capture the radiation emitted by the object under consideration, convert them into electrical signals and they are further processed to be displayed as temperature data.

(a) (b)

Figure 4-1: Vehicles used for data capture (a) Dodge RAM 3500 van (b) Ford Taurus car..

Real time thermal data capture requires the use of the thermal cameras, Indigo Omega Camera [Omega] and Raytheon Palm IR PRO Camera [Raytheon], Raytek Mx+4 infrared thermometer and Sony DV camcorder for data capture.

Omega is a long-wavelength camera (7.5 to 13.5 microns), which provides high performance thermal imaging. It has uncooled microbolometer detectors combined with on focal-plane signal processing which produces uncompromising image quality and incredible thermal resolution. Omega has an image optimization system which pre-processes image data and eliminates the need for temperature stabilization of the array. This enables Omega to operate over a wide temperature range with less power consumption and enables the absence of thermoelectric (TE) cooler which is conventional in uncooled cameras to hold the focal plane array at a stable temperature to avoid non-uniformly varying output which causes undesirable image artifacts. The absence of a TE cooler results in fast turn-on time, nearly 2 seconds for the initial image. Omega [Indigo], shown in Figure 4.2 (a), provides advanced camera control through an RS-232 serial interface. This can be accessed using a PC with either the standard serial communications port or the I/O module or using a high speed FireWire (IEEE-1394) serial bus and the FireWire module.

The Raytheon Palm IR PRO shown in Figure 4.2 (b) is a portable, hand held thermal imaging system [Raytheon]. It translates the infrared energy into electric signals and can be used as a night vision system. All objects emit differing amounts of infrared energy according to their temperature and characteristics. Raytheon uses this principle of varying temperature to view the object. The sensors in the camera convert the differing amount of thermal energy into equivalent amount of light energy. This capability causes the camera to capture the images of the objects by observing the thermal properties of objects in any light condition. The Raytheon camera has better resolution in image size compared with the Omega camera.

(a) (b)

Figure 4-2: The cameras used for thermal image acquisition (a) Indigo Omega Camera (b) Raytheon Infrared Camera.

The auto gain or the smart mode can be cancelled with the help of control panel software provided by the Indigo systems, which is not the case in Raytheon infrared camera. It is observed that the Omega camera is very sensitive to minute changes in temperature.

The setup for data capture is done as shown in Figure 4.3. The Dodge RAM vehicle used for data capture was first jacked up using a jacking lift. The two cameras mentioned earlier were mounted on tripods and the system was adjusted to focus the under vehicle chassis which was subdivided into three sections to get a complete view of the entire chassis. The real time thermal image sequences from the cameras were recorded continuously over a period of time. The Indigo Omega camera's output was recorded using a Toshiba laptop with the help of a frame grabber card as a video sequence. The Raytheon camera output was recorded as a video sequence using the Sony DV video camcorder through the normal audio/video output.

The first section of the Dodge van under vehicle chassis includes the catalytic converter and the muffler along with the other parts shown in Figure 4.4 (a). Similarly the first section of the Ford Taurus vehicle included the exhaust manifold pipes and the catalytic converter as shown in Figure 4.4 (b).

Figure 4-3: Hardware setup for thermal data acquisition. The setup includes the two uncooled infrared cameras, infrared thermometer and the laptop for controlling the devices.

(a) (b)

Figure 4-4: Visual images of Section I (a) Dodge van section involving the catalytic converter and the muffler (b) Ford car section involving the exhaust manifold pipes and catalytic converter.

The vehicle used for data acquisition was started at time 0 and left running until the entire sequence of 50 minutes was imaged. The starting room temperature was 30 degree Celsius. The set up was similar to the one used for Dodge van. The vehicle was jacked up and the engine was left running for the period of data capture.

The image sequence was acquired starting from time 0 when the engine was started and captured until 50 minutes using the Indigo Omega Camera and for a period of 30 minutes starting from time 0 using the Raytheon IR camera. The thermal image sequences from omega camera are included here for reference.

A complete thermal video was obtained using the two cameras. The video file was then edited and frames extracted from the video are represented here. The grayscale images were color coded using **MATLAB**. The sequence of images shown in Figure 4.5 (a - h) are color coded thermal image sequences of the first section of Dodge Van and Ford car, when the engine was started at time 0 with an interval of 2 minutes. As seen from the images for the Dodge Van, the pipe from the exhaust manifold is at higher temperature and is represented by red and the catalytic converter is in turquoise and represents less temperature value in the temperature scale. The muffler is even colder and is shown in dark blue which represents cold in the color scale. For the Ford car, we can see the changes in temperature over the catalytic converter surface. The exhaust manifold pipes are at higher temperature and they appear red due to the color scale used.

Scanning through the sequences, shown in Figure 4.5 [a –h], the variation in temperature can be clearly seen in the color coded images were the varying colors represent the change in temperature. The color scale used spans from blue, representing regions that are cold and red, representing regions that are hot. The change in temperature is caused by the exhaust gas flowing through the exhaust system and the result of convective heat transfer to the surrounding solid components.

The capturing of thermal image sequences for a period of time is a dynamic experiment in the sense that the experiments cannot be done continuously for all the sections. Before starting the imaging of second section, the vehicle engine has to be cooled completely. The cooling time of the vehicle takes more than two hours. The second section of the Dodge van under vehicle chassis to be imaged includes the muffler, drive shaft and the axle along with the other parts shown in Figure 4.6 (a). The jacked up Ford car was also cooled down to room temperature and the second section involving the muffler was imaged from time 0 to time 50 minutes. The Ford car was divided into only two sections due to the under vehicle chassis setup. The Catalytic converter was near the front side and the muffler was at the rear end of the chassis. The other automotive components were hidden and were not visible. Hence only two sections of the car were imaged. The Ford car's second section involving the muffler and the pipes from the catalytic converter are shown in Figure 4.6 (b)

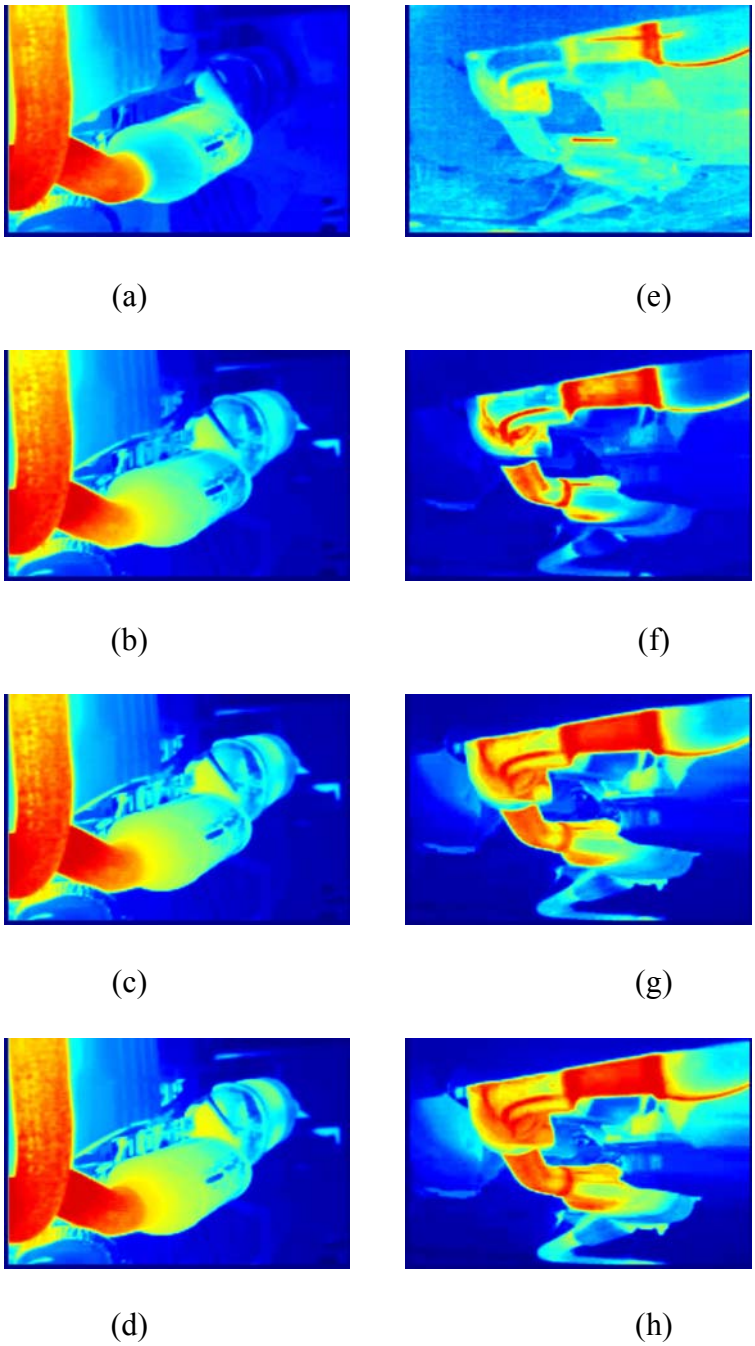

Figure 4-5: Thermal image sequences of Section I of Dodge Van and Ford Car. (a – c) Color coded thermal images of Dodge Van with an interval of 2 minutes (d – f) Color coded thermal images of Ford Car with an interval of 2 minutes.

(a) (b)

Figure 4-6: Visual images of Section II (a) Dodge van section involving the muffler, drive shaft and axle (b) Ford car section involving the exhaust pipes and muffler.

The thermal image sequence was acquired starting from time 0 when the engine was started and captured until 50 minutes using the Indigo Omega Camera and for a period of 30 minutes starting from time 0 using the Raytheon IR camera as described earlier. The thermal images included here are from Omega camera sequence. Thermal image sequences with an interval of 2 minutes of the both the vehicles are shown in Figure 4.7(a - h). The difference in the scene temperature can be observed by comparing the frames taken at time 0 and taken after 2 minutes and so on.

The axle and drive shaft surfaces in the Dodge van do not show any significant change in temperature and a conclusion can be drawn that the surface temperatures of the axle and drive shafts are normally cold compared with the muffler temperature. This conclusion helps us in identifying any abnormal surface temperature variations around these automotive components, which could be the result of a hidden threat object. These situations are discussed and the experimental results are shown in section 4.3.

The Ford car muffler surface temperature variation can be observed by scanning through the sequence of images in Figure 4.7 [e-h], represented as blue at time 0 and as yellow and/or red after 8 minutes. As discussed earlier in this section, the flow of exhaust gas causes the change in temperature on the muffler surface. It can be seen that the surface of the muffler closer to the catalytic converter is hot whereas the other end is not hot. The vehicle was again cooled completely before the third and the final section of the under vehicle chassis was imaged.

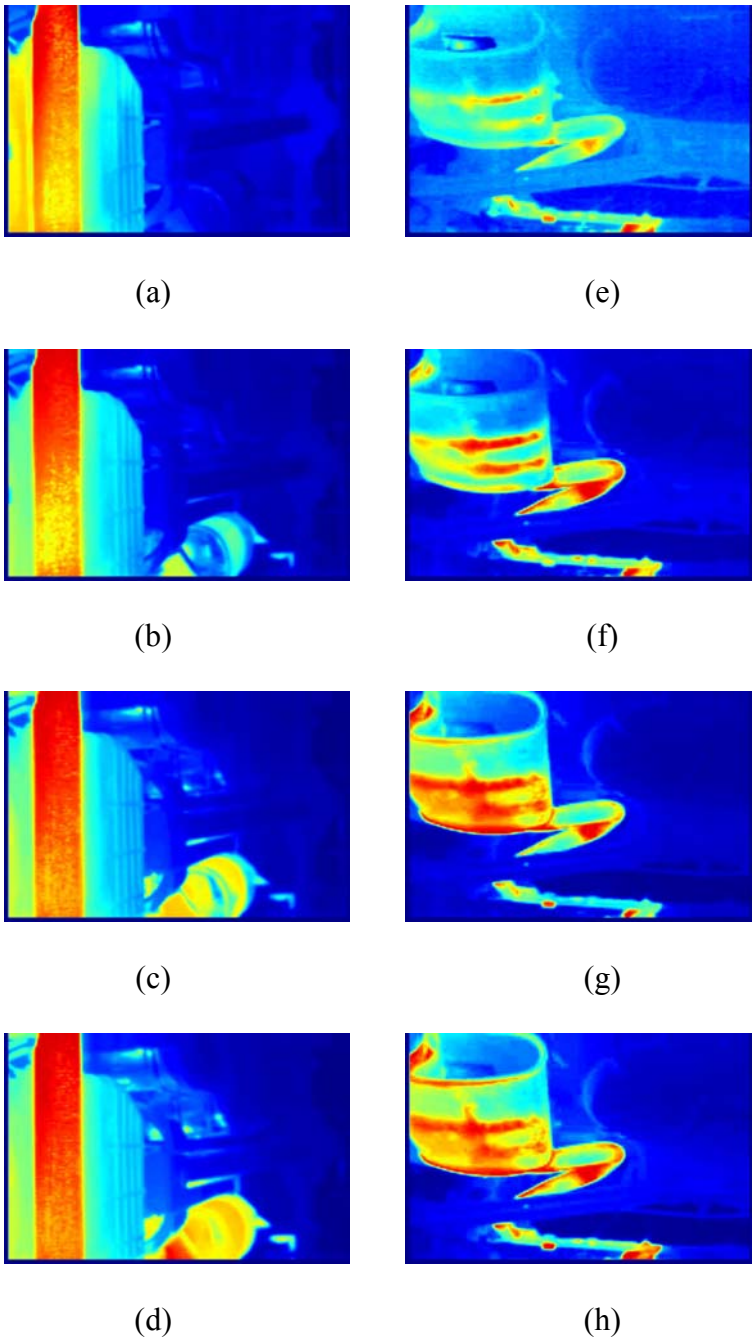

Figure 4-7: Thermal image sequences of Section II of the Dodge van and Ford car. (a – d) Color coded thermal images of Dodge van with an interval of 2 minutes (e – h) Color coded thermal images of Ford Car with an interval of 2 minutes.

The third section of the under vehicle chassis includes the tail pipe in the foreground and part of the muffler in the background as shown in Figure 4.8. As mentioned earlier the Dodge van engine was allowed to cool completely after taking the second sequence for two hours and the engine was started again to capture the variation in temperature starting from time 0 for the third section. There was no third section for the Ford Car. Hence the gray scale images are included here for the Dodge Van in Figure 4.9. The thermal image sequence was recorded as video starting from time 0 when the engine was started and captured for 50 minutes using the Indigo Omega Camera and for a period of 30 minutes starting from time 0 using the Raytheon IR camera.

The thermal image taken at time 0, shown in Figure 4.9 (a) and (e) infers that the tail pipe is at lower temperature compared with the background that appears red, representing that the area is hot. The exhaust gas flowing through the exhaust system takes a time of nanoseconds to reach the tail pipe and hence the first frame appears to be cold. The thermal image sequences in Figure 4.9 (b - h) show that the tail pipe has undergone change in temperature due to the flow of the exhaust gas. It can be inferred that the pipe surface is not homogeneous in temperature. The part of the tail pipe close to the muffler appears hotter compared to the end of the tailpipe, the change in temperature is due to the loss in pressure and temperature as the gas rushes out of the muffler through the tail pipe.

The exhaust system is the only system which is considered to be very hot in the under vehicle chassis, since there is no cooling agent in this system. This is proved true by the thermal images shown here. The exhaust system components are expected to be very hot based on these results. Hence if they appear to be cold over a period of time or show any changes in their temperature signature, then they should be inspected for any threats. These expectations are basis for the threat detection section 4.3, which inspects the under vehicle chassis to meet the basic expectations and looks for other unusual objects.

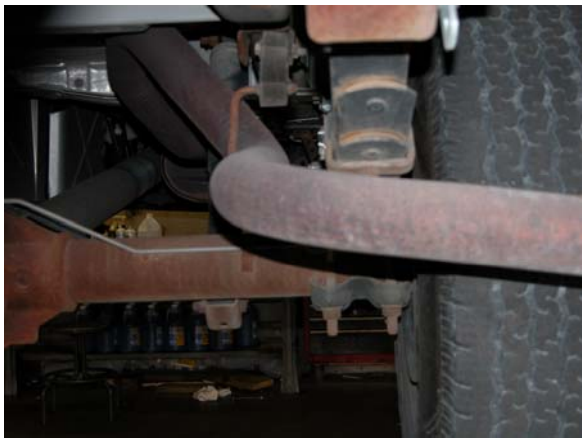

Figure 4-8: Visual image of Section III of Dodge van involving the tail pipe.

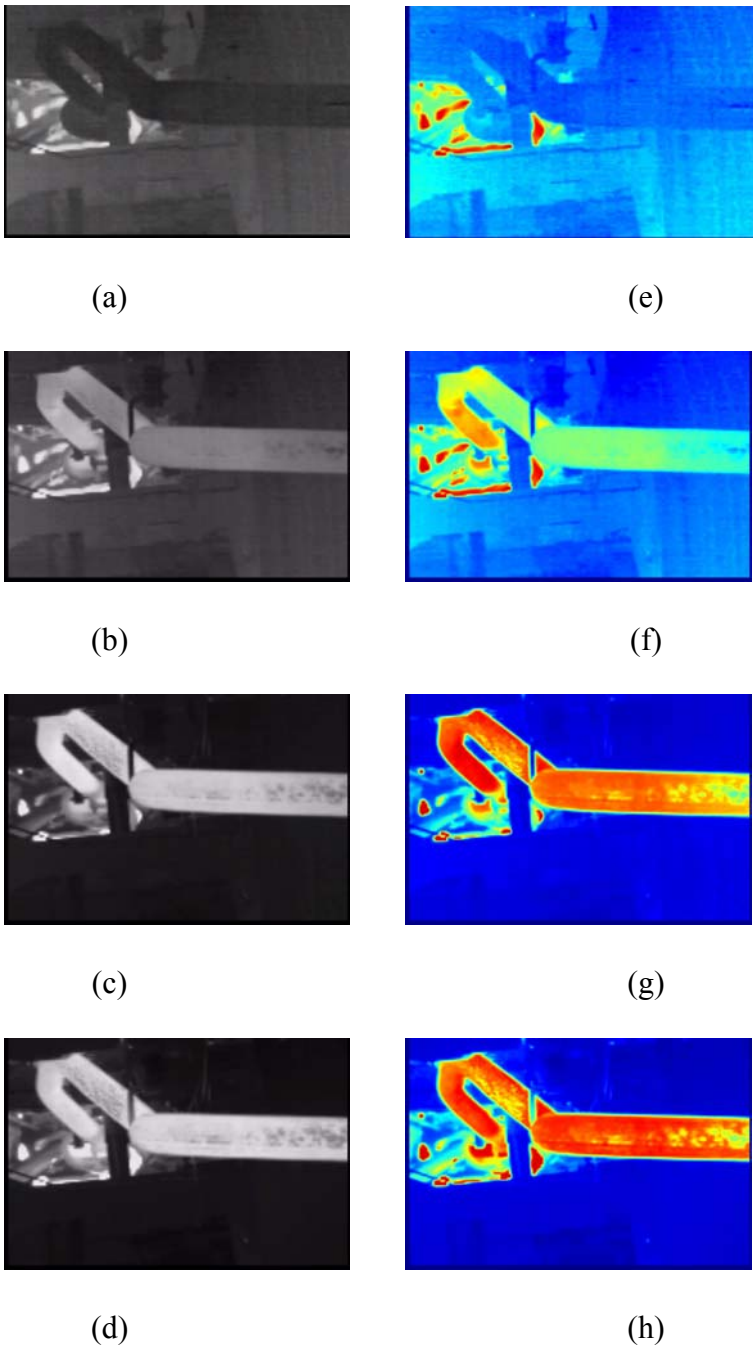

Figure 4-9: Thermal image sequences of Section III of Dodge van involving the tail pipe. (a – d) Gray scale thermal images with an interval of 2 minutes (e – h) Color coded thermal images with an interval of 2 minutes.

4.2 Temperature Measurement Using Infrared Thermometer

This section details with the measurement of temperature using the infrared thermometer. The thermometer measures the amount of infrared energy emitted by a target object and calculates the temperature of that object's surface. For better simulation results, it is necessary to provide the exact temperature values or curves of the automotive parts under consideration. Up to date the temperature curves used for simulation where assumptions [Srinivasan, 1995], hence this necessitates the measurement of temperature over a period of time for improved thermal modeling. The thermal modeling software MuSES has to options for temperature assignment namely the value or the curve. Real time temperature curves are measured using the infrared thermometer shown in Figure 4.10[Raytek].

The thermometer provides real time continuous data capture through RS232 serial output when connected to the computer. The MX4+ thermometer can be used to monitor, graph, and record real-time temperature changes with the DataTemp software. The software provides a convenient way to export temperature data files in a format that can be used by programs such as Access, Excel, and condition monitoring programs. The temperature values up to 100 data points can be logged into the thermometer and the data logging feature enables to see temperature trends and potential equipment problems by graphing data accumulated.

The hardware setup for temperature measurement is the same as described in section 4.1. The thermometer when connected to the Toshiba laptop continuously records the temperature values of a particular automotive part over a period of time that can be specified using the interactive software.

Figure 4-10: Raytek Mx4+ infrared thermometer used for temperature measurement.

The recording interval for temperature measurement can also be specified. It can vary from 0.125 seconds to 1 minute. The experimental results are shown and discussed later in this section. The temperature data obtained using the thermometer is used for the simulation of thermal images of under vehicle automotive parts. CAD models or laser scanned and reverse engineered models are used for simulation and thermal properties are assigned based on the temperature data obtained over a period of time.

For the experiments, the thermometer was mounted onto the tripod and the laser trigger was locked for continuous measurement. The measurement interval was set as 0.125 seconds. The thermometer was connected to the laptop through the serial port and the data was recorded as a graph in the interactive software that came along with the thermometer. The thermometer was focused on to a particular point on the automotive part surface and the temperature was measured for a period of 30 minutes. The vehicle used for data capture was left running during the time of capture of temperature data.

The exhaust system components are the ones that show a significant variation of temperature with respect to time as the exhaust gas flows through the system. The exhaust system components selected for measurement were the catalytic converter, the muffler, the tail pipe and the transmission. The temperature data obtained as a graph can be exported as a text file. The export parameters can be set using the export setup option in the software provided. The exported text file is imported into Matlab for fine tuning of the resulting plot. The point of measurement of temperature on the surface on the catalytic converter is highlighted in the Figure 4.11. The resulting temperature graph is shown in Figure 4.12. The graph time starts from time 0 and ends at time 30. The time displayed in the graph is the actual time the engine was started and stopped.

Figure 4-11: Catalytic converter of the Dodge RAM 3500.

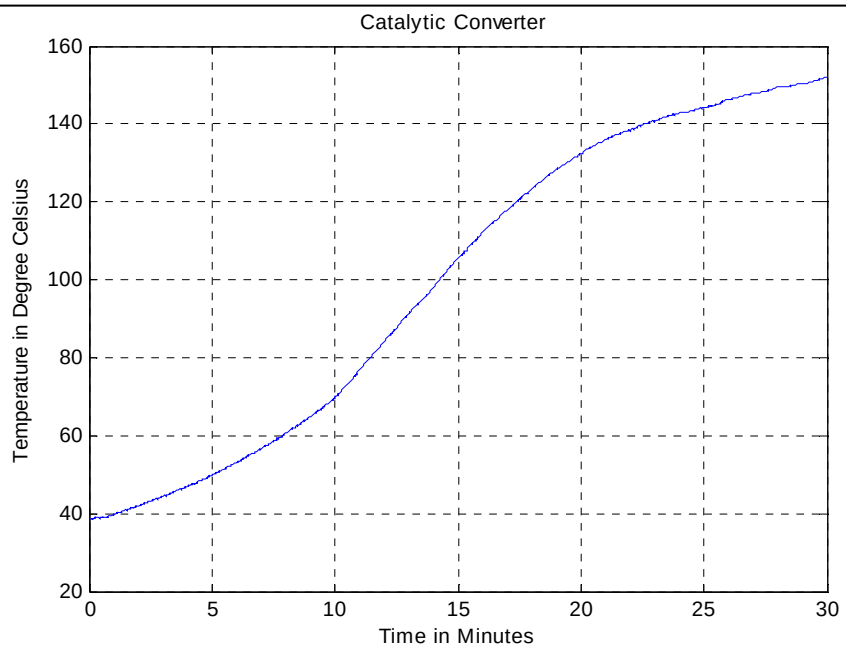

Figure 4-12: Graph showing the temperature measurement of the catalytic converter for a period of 30 minutes.

The starting temperature of the catalytic converter is above 30 degree Celsius and the temperature after 30 minutes is 152.8 degree Celsius. The room temperature was 30 degree Celsius. The vehicle was jacked up and was made to run at idle without changing the engine power or rpm.

The experiment conducted here is a dynamic experiment, for capturing the temperature data from the initial room temperature to a period of 30 minutes, necessitates the cooling of the vehicle after one complete set of data is taken for a particular automotive part. The engine was stopped and left to cool for a period of one to two hours and then the experiment was repeated for the rest of the components to be measured. The muffler surface temperature was also measured in a similar way as described earlier.

The geometry and the corresponding temperature curve of the automotive component vary for different models of the automobile. For simulation of thermal images it is necessary to have the CAD model of the automotive component and the temperature curve of that component for a particular type of vehicle.

The point of measurement of the Dodge RAM 3500 van muffler is shown in the Figure 4.13 (a). The muffler actually varies in temperature along its surface. The assumption here is that the part of the muffler closet to the catalytic converter receives more heat and the other end is at a lower temperature compared to the front end. The middle part of the muffler has significant temperature variation and is higher than the front and the rear end surface of the muffler. The starting temperature of the muffler when the vehicle was started is 24.0 degree Celsius that can be inferred from the temperature curve given below. The room temperature was 25.0 degree Celsius. The muffler geometry varies between cars from different manufacturers. For getting a better idea about the temperature curve of different mufflers, the Ford Taurus muffler surface temperature, shown in Figure 4.13(b), and the Toyota Corolla Muffler surface temperature, shown in Figure 4.13(c), were measured The muffler surface was divided into three regions namely the front region, the side closer to the catalytic converter, middle region and the rear region, the side closer to the tail pipe. Similarly the Dodge RAM muffler was divided into three regions and the temperature curve was measured. The resulting temperature graphs are shown in Figures 4.14, 4.15, and 4.16.

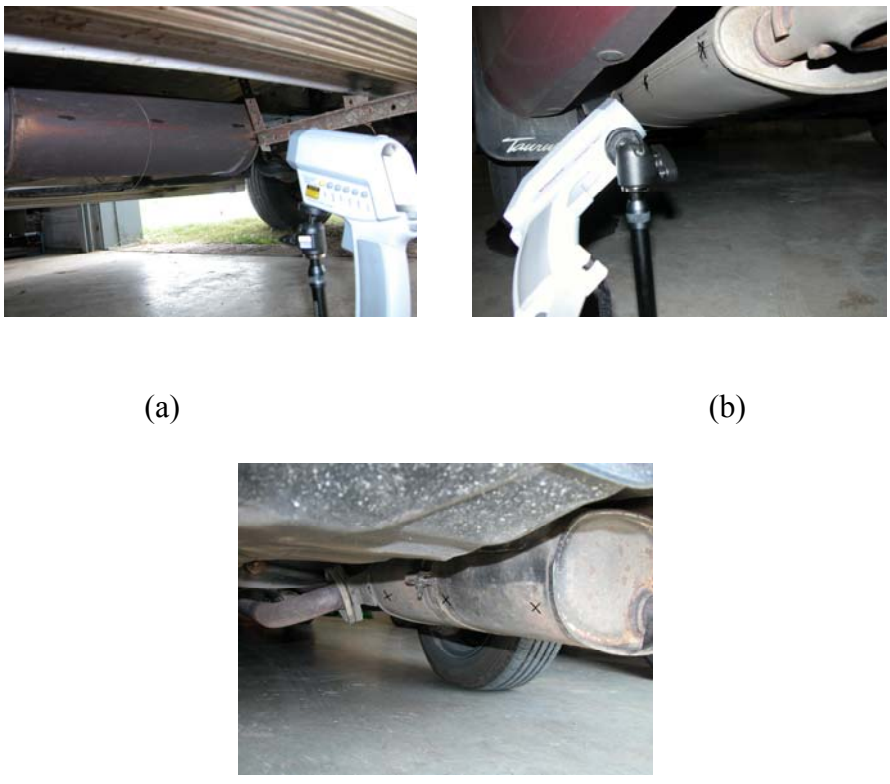

Figure 4-13: Muffler with the point of measurement highlighted. (a) Muffler of Dodge RAM 3500 Van (b) Muffler of Ford Taurus and (c) Muffler of Toyota Corolla.

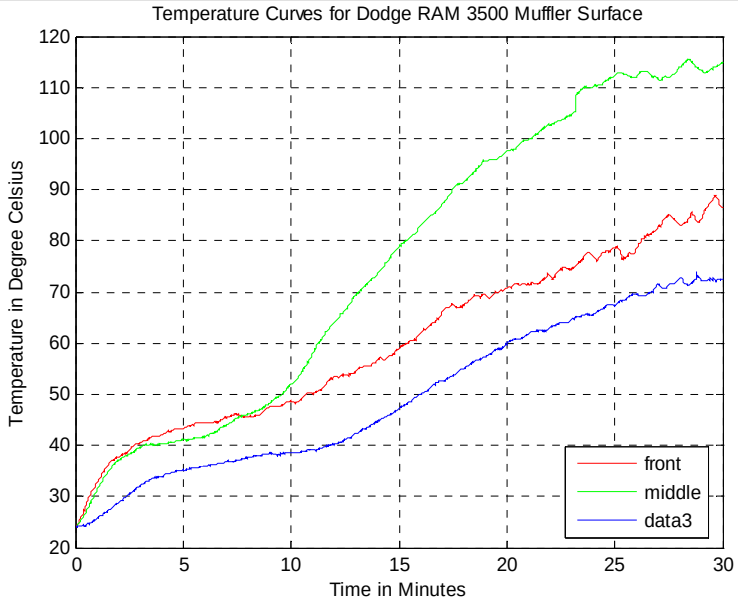

Figure 4-14: Graph showing the temperature measurement of the muffler for a period of 30 minutes.

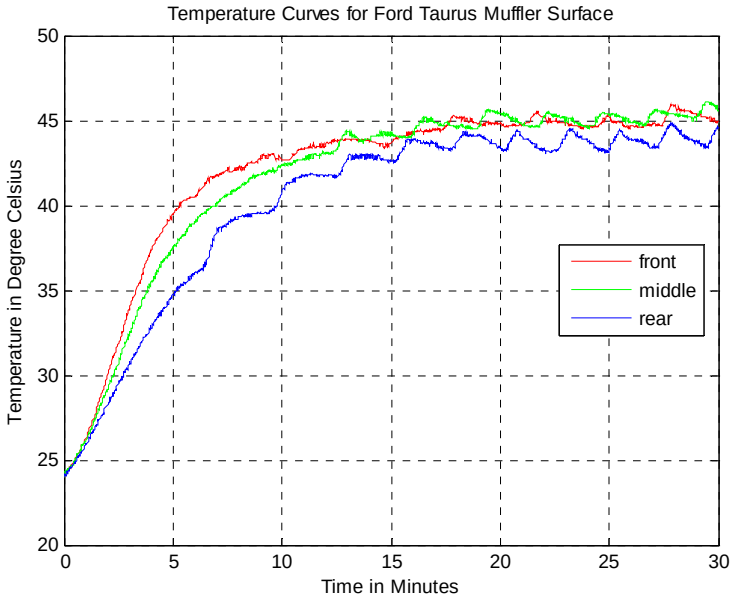

Figure 4-15: Temperature curve of Ford Taurus muffler (front end, middle and rear end) for a period of 30 minutes.

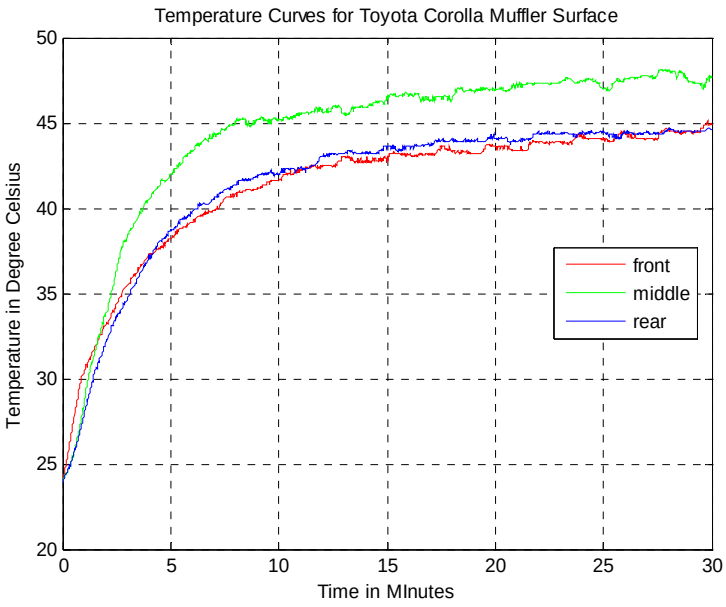

Figure 4-16: Temperature curve of Toyota Corolla muffler (front end, middle and rear end) for a period of 30 minutes.

It can be inferred from the above graphs that the muffler surface temperature is not the same for all cars. The geometry of the mufflers is different which can be inferred from Figure 4.13 and the engine capacity varies between the three vehicles selected for experimentation. The Toyota Corolla has a V4 engine, Ford Taurus has V6 engine and the Dodge RAM has V8 engine. The volume of exhaust gas flowing from the engine will be more in Dodge RAM vehicle and the temperature values vary based on the gas flow for a period of 30 minutes. The maximum temperature reached by Dodge RAM muffler surface is 120 degree Celsius whereas Toyota Corolla muffler reaches only 46 degree Celsius in 30 minutes. For thermal modeling of automotive parts of different vehicles it is necessary to use the corresponding 3D model of the vehicle and the temperature curve of the automotive components of that particular vehicle. Similarly the experiment was done for the tail pipe. The resulting plot is given in Figure 4.17 and the starting temperature of the tail pipe is close to 30.2 degree Celsius and the temperature after 30 minutes is 94.3 degree Celsius. The temperature curves obtained as a result of experiments conducted are used as basis curves in the simulation of thermal images of the automotive parts in the software MuSES.

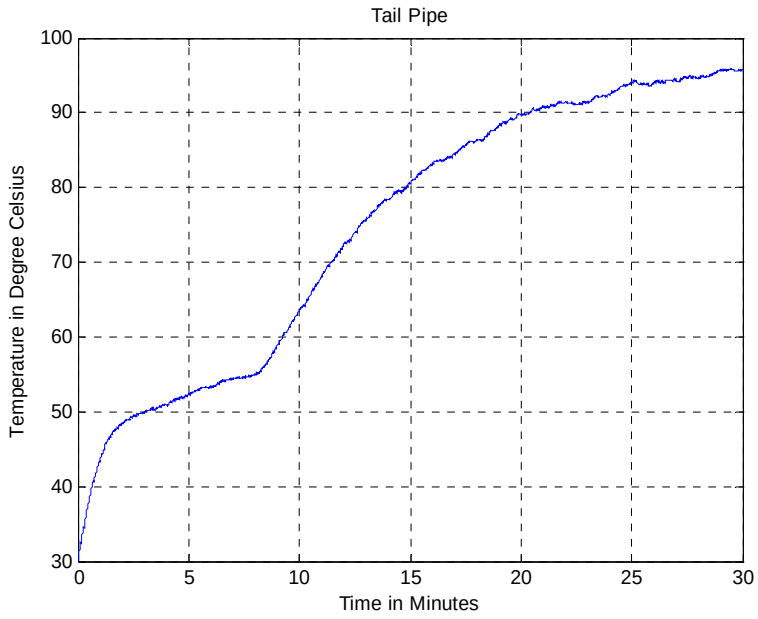

Figure 4-17: Graph showing the temperature measurement of the tail pipe for a period of 30 minutes.

4.3 Thermal Images for Threat Detection

This section discusses the change in the heat pattern of the thermal images of automotive components when something unusual is present in the under vehicle chassis other than components shown in Section 4.1. The thermal sequences with unusual objects were captured to observe the variation in the thermal image which identifies the abnormality in the under vehicle chassis and aids in inspection and in turn results in security and surveillance.

The data capturing setup is the same as explained in Section 4.1 except for the Raytheon camera. The Indigo Omega camera was only used which was connected to the laptop for acquiring the sequence of thermal images of the unusual automotive parts. The objective of this sequence is to identify the components that are not normal. The basic idea for this inspection is expectation and hidden threat objects. These assumptions and expectation are inferred from the thermal data sequences collected under normal conditions, the results of which were discussed in Section 4.1.

Exhaust system components like muffler, catalytic converter are inspected in the following experiments for their normal temperature variation and are expected to be hot surfaces. Any change in surface temperatures or no variations in their temperature pattern are considered to be suspicious and the components are subject to further inspections. Similarly, surfaces of gas tanks or drive shafts are expected to be cold when compared with the near by muffler or catalytic converter surface temperature. Change in their surface temperature makes them appear hot in the thermal image and then they are considered to be suspicious and are subject to inspections. Another setup looks for threat and/or unusual objects hidden in cavities or other places that cannot be seen in a visual image but can be seen in the thermal image due to either heat pattern.

Inspecting under vehicle chassis for threat objects such as car bombs, and other kinds of hidden threat objects that are unusual in the normal scene has become necessary due to terrorist attacks. Visual images may not be able to identify the nature of the hidden object. Things that seem to be normal in the visual band can be a threat object in the thermal band. The under vehicle chassis is inspected for changes in expectations of object's surface temperature for example, muffler surface has to be hot and gas tank surface has to be cold and also inspected for objects hidden in cavities which are not seen in the visual image.

The first setup involves the hooking up of a muffler which is not connected to the exhaust system of the under vehicle chassis, but is hanging in the under vehicle chassis appearing to be connected to the chassis. This muffler is referred as the false muffler and the real muffler being the one connected to the exhaust system of the vehicle used for data acquisition. The thermal sequence of the real muffler is captured using the Indigo Omega camera over a certain period of time to visualize the temperature changes with respect to time and the same procedure is done for the false muffler capture. Here the thermal sequence is captured only for a period of 2 minutes. The real muffler and the drive shaft are shown in Figure 4.18 and gray scale thermal image and color coded thermal images of the muffler are shown in Figure 4.19.

The entire sequence is recorded as a video and then the frames are extracted from the video. The muffler surface is slightly hot at time 0 and the surface temperature varies based on the exhaust gas temperature flowing through the muffler. The variation can be observed if and only if the muffler is connected to the exhaust system. The muffler shows variations in temperature with respect to time and this is the basic expectation of a muffler present in the under vehicle chassis. The increase in temperature on the surface of the muffler can be observed from the Figure 4.19 (c) and (d) extracted as a frame from the video after 2 minutes. The hot surface is represented bright in the gray scale image and red in the color coded thermal image.

Figure 4-18: Visual image showing the real muffler connected to the exhaust system.

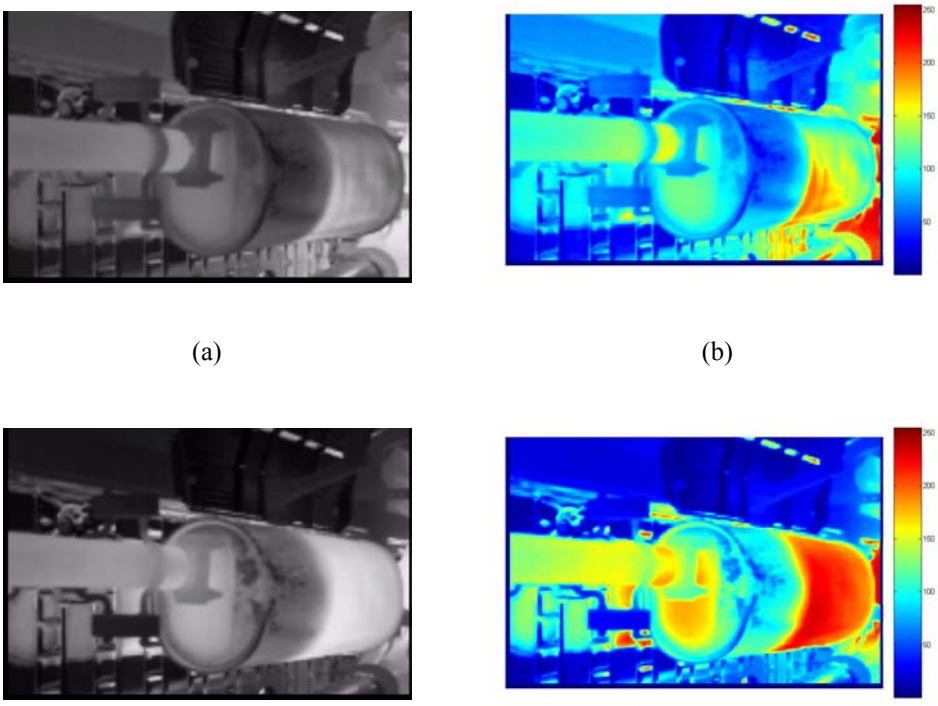

(a) (b)

(c) (d)

Figure 4-19: Thermal image of real muffler. (a) Gray scale thermal image at time 0, (b) Color coded thermal image at time 0, (c) Gray scale thermal image at time 2 minutes, and (d) Color coded thermal image at time 2 minutes.

The false muffler attached to the under vehicle chassis but not connected to the exhaust system is shown in Figure 4.20. The experiment is repeated with the camera now focusing the false muffler for a specified period of time. The resulting real time thermal image sequence is recorded as video for a period of 2 minutes.

The resulting gray scale and color coded thermal images are shown in Figure 4.21[a –b]. It is inferred from the thermal image that the muffler appears gray in the gray scale image and blue in the color coded image, which represents that the muffler is cold and is not showing any increase in temperature.

No change in temperature is against the basic expectation of a muffler present in the under vehicle chassis, that the muffler should be hot when connected to the exhaust system. The thermal image shown in Figure 4.21[c–d] that was taken after 2 minutes also does not show any variation in temperature. The inference is that the muffler has to be inspected and when it is inspected, it will be evidently clear that this muffler was not connected to the exhaust system of the vehicle and is nothing but a threat object. It can then be disconnected and inspected for the presence of weapons.

The original muffler connected to the exhaust system components shows temperature variations with respect to time as the exhaust gas flows through it whereas the false muffler doesn't show any variations because there is no exhaust gas flow through it. Hence, even though in the visual image both mufflers do not arise any suspicious thinking, the thermal image of them clearly shows that the second muffler is highly suspicious.

Figure 4-20: Visual image showing the false muffler.

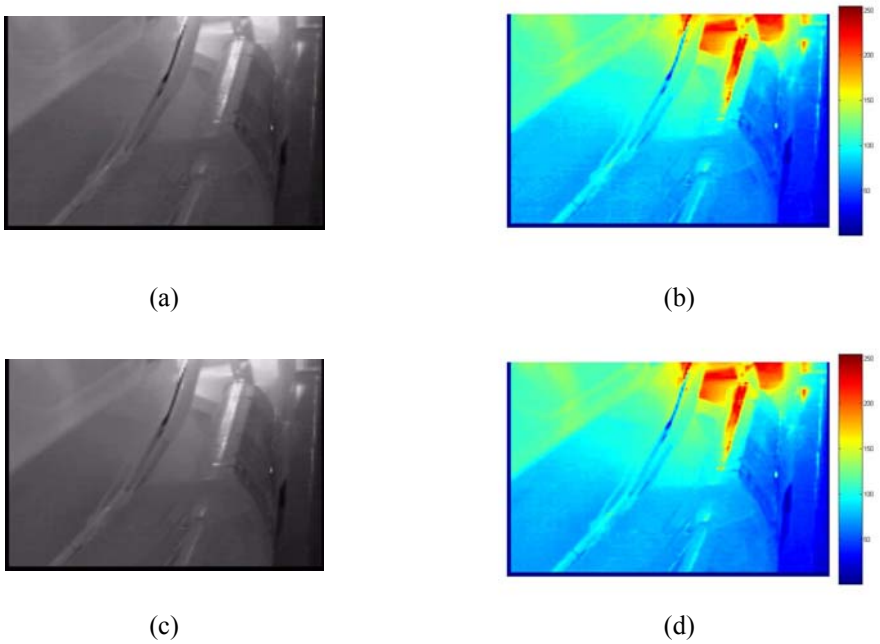

(a) (b)

(c) (d)

Figure 4-21: Thermal image of the false muffler at time 0. (a) Thermal image at time 0 (b) color coded thermal image at time 0(c) Thermal image at 2 minutes (d) color coded thermal image at 2 minutes.

The second scenario for threat detection includes the search of objects that are hidden or placed in such a way that they are not identified as a threat object in the visual image. Such objects merge with the background around the exhaust system components or other under vehicle automotive components. The Ford Taurus vehicle was used for data capture by setting up objects not detectable in the visual images. The box is placed in such a way that it merges with the background. The object was placed near the catalytic converter and near the gas tank. The catalytic converter normally appears hot due to the flow of exhaust gas whereas the area surrounding the gas tank is at a lower temperature compared with the catalytic converter. The experimental setup (visual images) and the resulting thermal images are shown in Figure 4.22 (a) and (b) for catalytic converter and in Figure 4.23 (a) and (b) for the area surrounding the gas tank. It can be clearly observed that the hidden box, which is not easily detectable in the visual image, is identified as a threat object when seen through an infrared sensor. Similarly the object placed on the cavity near the gas tank is also identified as a threat object with the help of thermal imaging. These examples illustrate the application of thermal imaging in the field of threat detection.

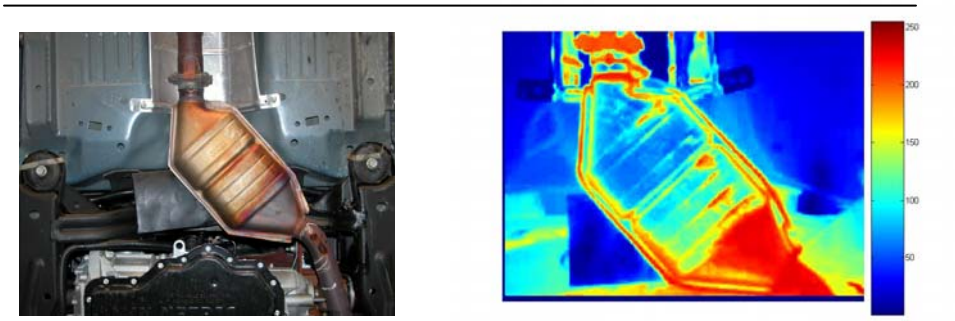

(a) (b)

Figure 4-22: (a) Visual image of the catalytic converter with an undetectable threat object. (b) Thermal image of the same scene with an identified threat object.

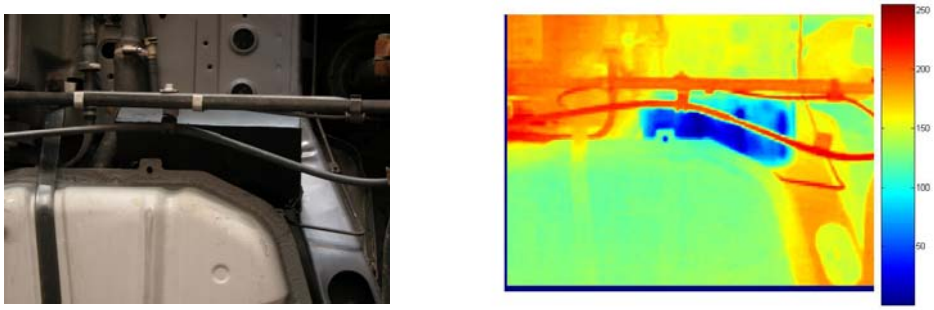

(a) (b)

Figure 4-23: (a) Visual image of the catalytic converter with an undetectable threat object. (b) Thermal image of the same scene with an identified threat object.

The experimental results obtained in section 4.1 and section 4.2 are incorporated in to virtual simulation of thermal images using the software MuSES. They serve as a ground truth for validation and calibration. The exact temperature curve if measured for all the automotive components in the under vehicle chassis can be used to obtain better improved simulation results. The measurement of temperature of all components is a tedious task since it involves the placement of the sensor in areas that cannot be reached easily. The surface temperatures of the parts depend on other factors that take place internally and they may not be the same always. The experiments that were done for threat detection highlight the advantage of thermal image inspection to visual image inspection and due to increasing threat attacks, it becomes necessary to inspect the vehicles in both the visual and infrared bands.

.

5 EXPERIMENTAL RESULTS - SIMULATION OF SYNTHETIC THERMAL IMAGES

This chapter discusses in detail the experimental results obtained for simulation of thermal images using the software MuSES. The simulation results of models that were created using 3D modeling tools are discussed in Section 5.1. Section 5.2 discusses the signature predictions of the CAD models. Finally Section 5.3 describes the simulation results of the reverse engineered automotive components.

5.1 Simulation of 3D Models created using Modeling Tools

This section describes in detail the experimental setup and the results for the 3D models created using the 3D modeling tools. The exhaust system model and the complete car model are described and the results are discussed and analyzed. The complete vehicle model is simulated for various experimental conditions. The models were created using the 3D modeling tool Rhinoceros® (Rhino), NURBS modeling tool for Windows. The 3D models are created as NURBS surfaces or polysurfaces in Rhino and are exported as polygon meshes that are suitable for simulation in MuSES.

Simulation of Exhaust System Model

The exhaust system is the only system which is at a high temperature due to the disposal of the engine combustion products. The exhaust system consists of the manifolds, catalytic converter, front pipe, muffler and the tail pipe. Each of the exhaust system components show a significant change in temperature, the real time results of which were discussed earlier in Section 4.1 and 4.2 of chapter 4.

The exhaust system model in Figure 5.1 consists of the floor pan, muffler, heat shield, inlet pipe and the tail pipe. The model was designed and carefully created using Rhino3d and the material properties and the bounding box parameters were set for each component in the model builder and are shown in table 5.1. The inlet pipe, muffler and the outlet pipe are set as assigned temperature parts and the temperature curves are assigned to the parts for a period of 15 minutes in an increment of 5 minutes.

Figure 5-1: Exhaust system model.

Table 5-1: Thermal properties assigned for the exhaust system model

Properties	Floor Pan	Inlet Pipe	Muffler	Heat Shield	Outlet Pipe
Part type	Calculated Standard	Assigned	Assigned	Calculated Standard	Assigned
Material	Steel (Mild)	-	-	Steel (Mild)	-
Thickness	1.5	1.5	1.5	1.5	1.5
Surface condition	Steel as Rcvd,0.74	Steel as Rcvd,0.74	Steel as Rcvd,0.74	Steel as Rcvd,0.74	Steel as Rcvd,0.74
Temperature	20 degrees	Inlet curve 250 degrees	Muffler curve 225 degrees	20 degrees	Outlet curve 200 degrees
Convection coefficient	50	0	0	50	0
Fluid flow temp	20	Ambient air	Ambient air	20	Ambient air

The results are expected based on the temperature curve assigned, the inlet pipe being the hottest and the floor pan to be coldest. Each and every element view factor rays were calculated and the numerical solution was done. The simulation results are shown in Figure 5.2 (a – d). The variation in temperature can be observed by scanning through the sequence of images. At the end of 15 minutes, the thermal analysis was done and the simulated thermal model output was given. The simulation time was expected to vary based on the complexity of the model mesh. The exhaust system model mesh was of less complexity and simulation was observed to be close to half an hour. The results can be exported or plotted and can be animated. Here the simulation result is found to be exact according to the temperature curve. The temperature ranges are given a specific color based on the color scale given in the image.

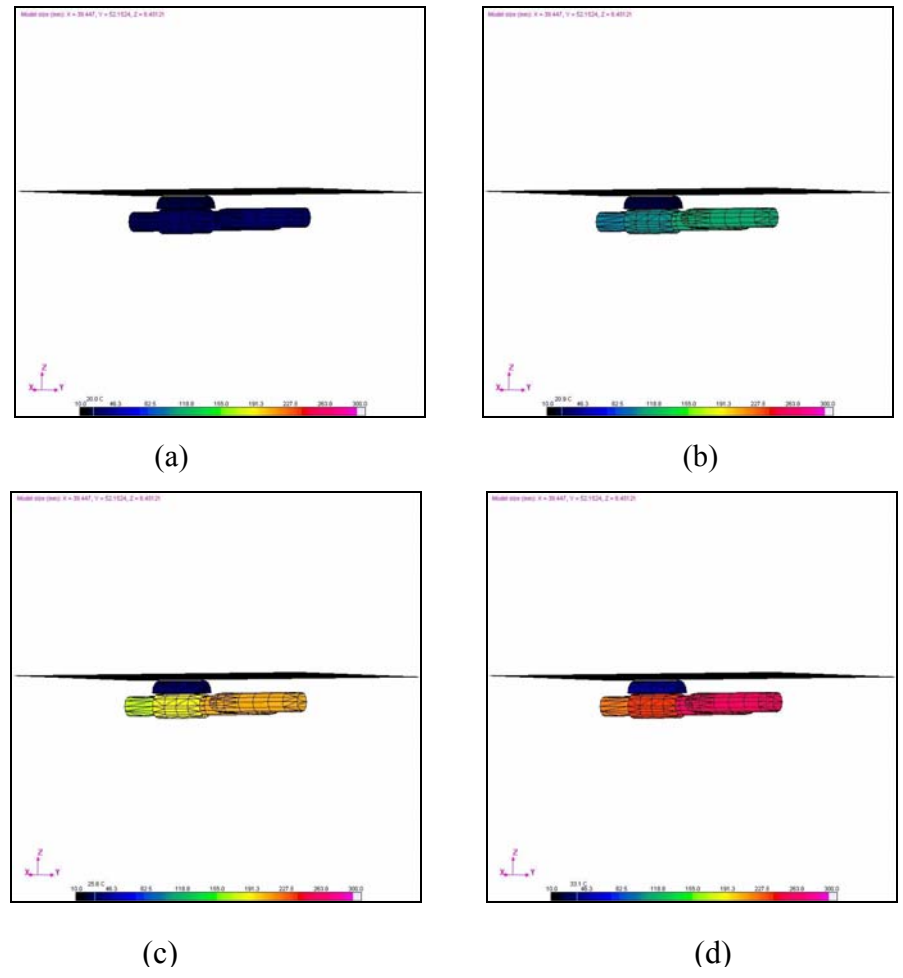

Figure 5-2: Simulated result of exhaust system. (a) Simulation result at time 0 (b) Simulation result at 5 minutes (c) Simulation result at 10 minutes and (d) Simulation result at 15 minutes.

Simulation of Complete Car Model

The complete car model was created such that all the under hood and under vehicle components are included. The complete car model is shown in Figure 5.3 detailing the automotive components included in simulation. The model is of medium complexity with the upper body and the under body of the car. The automotive components like radiator, air filter, air filter pipe, intake manifold, engine block and catalytic converter are included in the model. The 3D model was created as a NURBS surface in Rhino and was exported as polygon meshes. The polygon mesh was imported in to MuSES and the thermal properties were assigned.

All the parts were assigned as calculated thermal parts, except for the engine block and the four fluid parts that were created without any geometry. The fluid parts were virtually imagined as the exhaust gas fluid flowing through the exhaust system. The fluid parts were connected to each other through advection links and connected to the corresponding solid parts in the exhaust system through convection links.

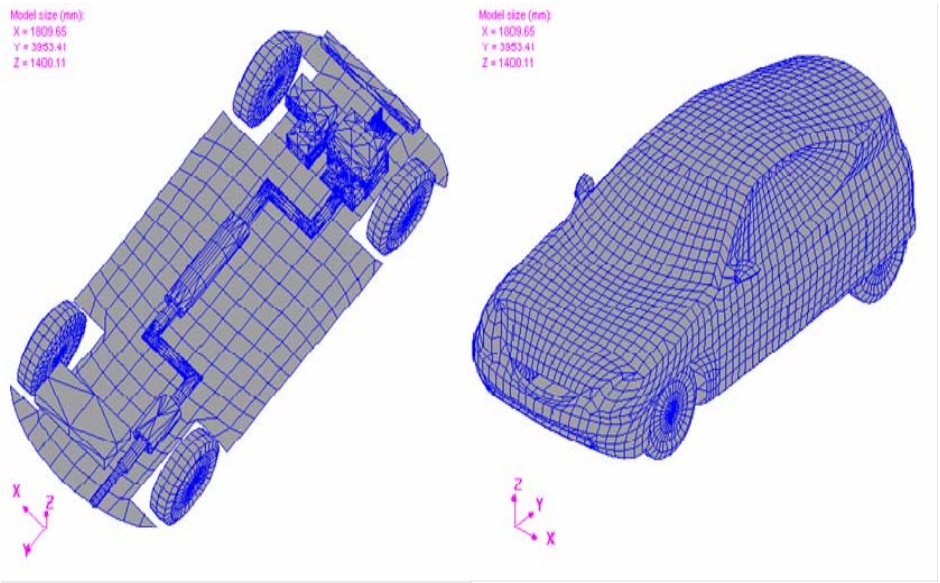

(a) (b)

Figure 5-3: 3D Model of complete car (a) Image showing car under vehicle chassis, (b) Image showing car upper body.

The four fluid parts created were the exhaust gas which was connected to the exhaust manifold through convection, front pipe exhaust gas connected to the front pipe of the muffler, muffler exhaust gas connected to the muffler and the rear pipe exhaust gas fluid connected to the rear pipe of the muffler. The exhaust gas was assigned a temperature curve as shown in Figure 5.4 and the other three exhaust gases were connected to the corresponding upstream fluids with a flow rate of 8000 L/min, a reasonable assumption. The exhaust gas temperature shown here is a best assumption from the knowledge gained from predictions and from online resources.

The engine block was assigned two temperature curves, one for the interior side of the elements and one for the outer side. The reason for such assignment is that the inside of the engine encounters the effect of pressured coolant fluid or oil that flow in the engine compartment and carry away most of the heat away and maintains the temperature of the engine at a certain temperature. The rest of the parts are set as calculated temperature parts and the environmental conditions are set based on the weather file dated July 19, 1984. The environmental file includes the values for wind direction, solar irradiance, humidity, cloud cover, and other related factors that affect the temperature of the automotive components. The simulation was carried out for a period of 15 minutes and the results are shown in Figure 5.5 (a – d) and 5.6 (a – d).

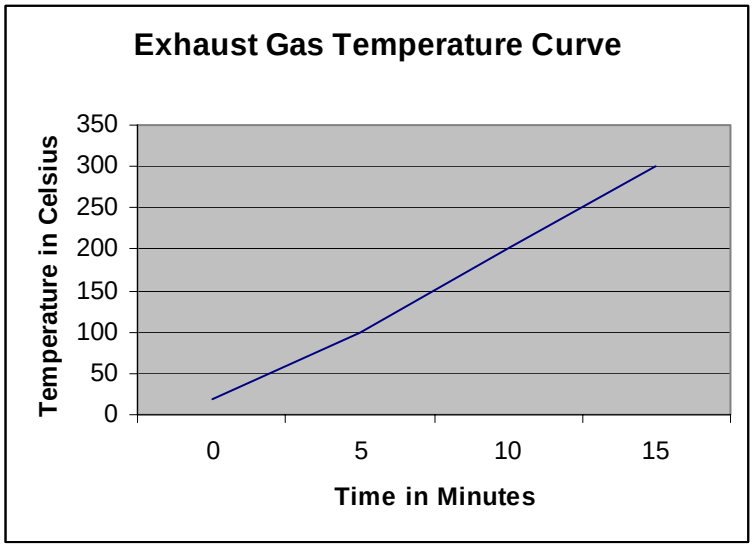

Figure 5-4: Exhaust gas temperature curve.

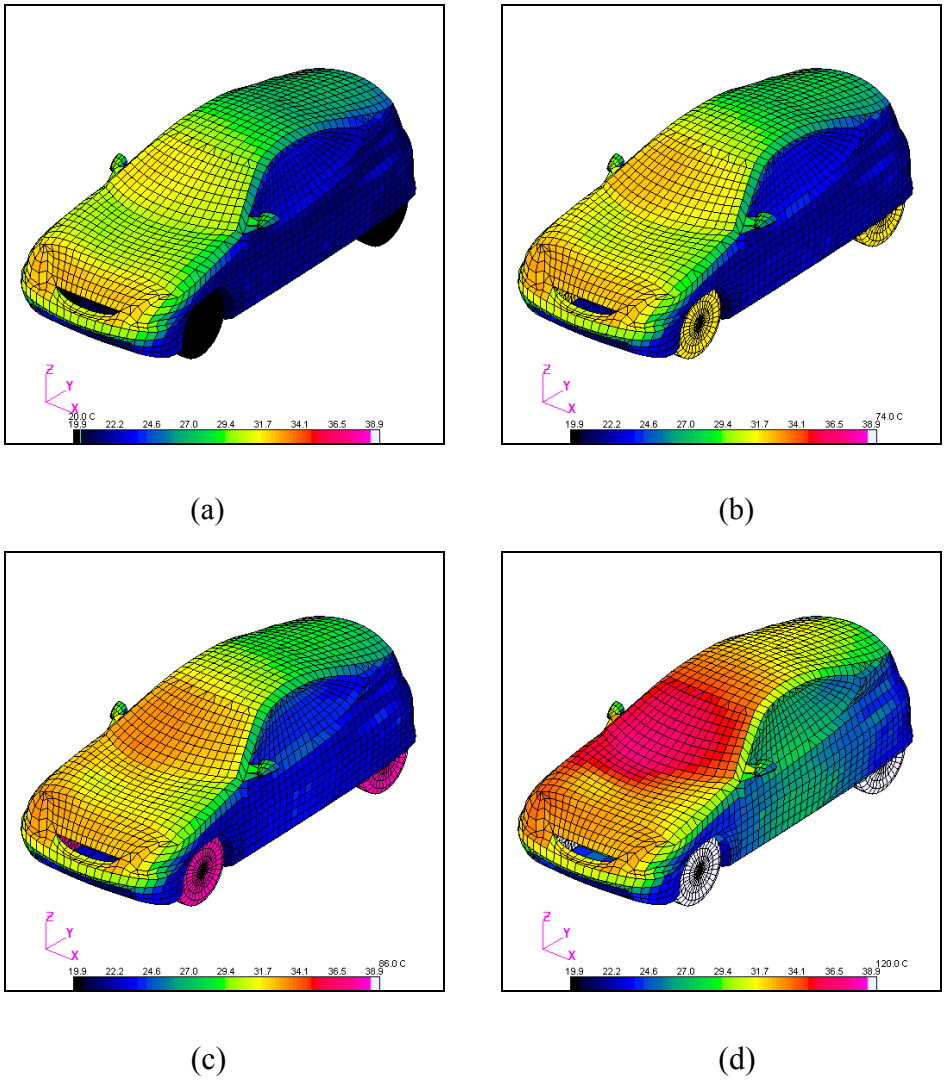

(a) (b)

(c) (d)

Figure 5-5: Simulated result of car upper body. (a) Simulation result at time 0 (b) Simulation result at 5 minutes (c) Simulation result at 10 minutes and (d) Simulation result at 15 minutes.

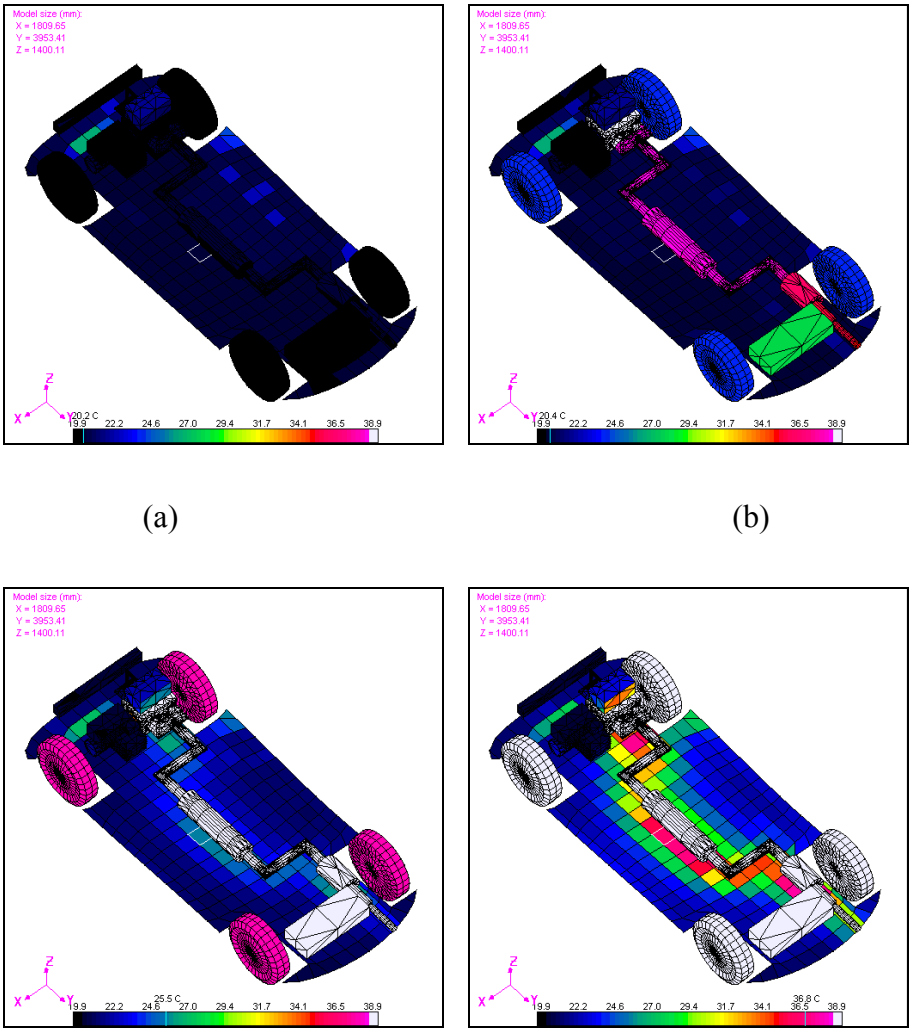

Figure 5-6: Simulated result of car under body. (a) Simulation result at time 0 (b) Simulation result at 5 minutes (c) Simulation result at 10 minutes and (d) Simulation result at 15 minutes.

The thermal modeling results were shown in Figure 5.5 (a – d) and 5.6 (a – d). The outer body or the upper body of the car was observed to be hottest in the region near the engine compartment and the temperature signature moderately spreading around the entire body, which can be inferred from the sequences of images shown. In the under vehicle chassis the resulting temperature of the components were observed to be based on the exhaust gas temperature. The basic assumption of the muffler surface from the inference of real time experimental results was that the front pipe of the muffler should be at a higher temperature than the muffler and the muffler should be at a higher temperature compared to the rear pipe of the muffler. The same pattern was observed in the simulation results. This effect happens in real time because of the pressure and temperature drop of the exhaust gas inside the muffler.

The components were given color based on the color scale below the image for a specific temperature in the scale. The components that are white are hotter and those that are in black are colder. The components get their temperature based on the heat conduction from the engine block and due to the flow of the fluids in the exhaust system. The resulting thermal images as seen through a sensor are shown in Figure 5.7 and 5.8. The thermal images were simulated based on the bidirectional reflectance distribution solution and the signature analysis done for multiple bands.

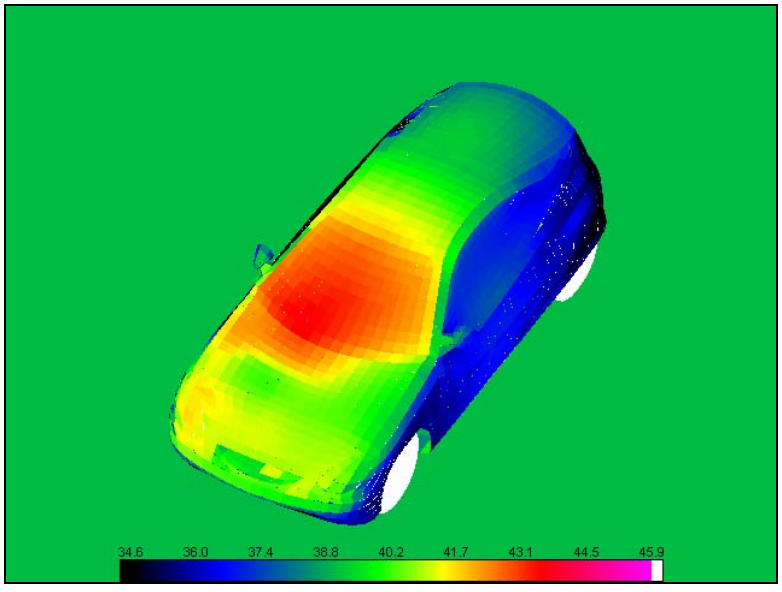

Figure 5-7: Simulated thermal image of car. The car is parked facing the sun and hence based on the environmental conditions; the body of the car appears very hot.

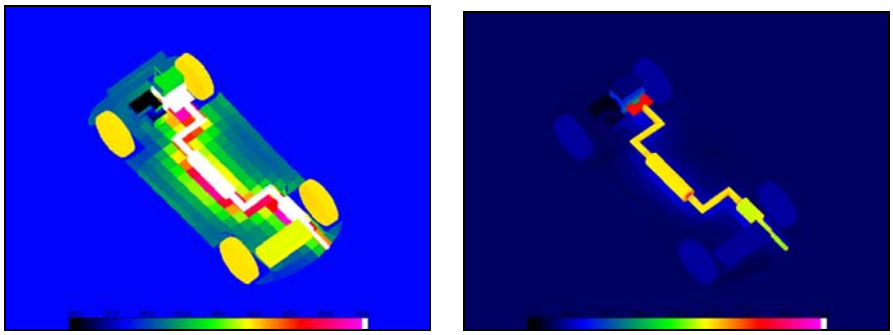

(a) (b)

Figure 5-8: Simulated thermal image of car under body chassis. (a) Highlights the lower temperature changes, (b) Highlights the exhaust system components temperature changes.

Simulation of 3D Model Incorporating Measured Temperature Curves

The measurement of temperature using the infrared thermometer was discussed earlier in Section 4.2 of Chapter 4. The temperature data acquired for a period of 30 minutes is used as a ground truth for simulation and is assigned to the corresponding automotive components and the resulting simulation results are discussed in this section.

The Dodge RAM 3500 vehicle shown in Figure 4.1 was used for the measurement of temperature data. The exhaust system of the vehicle consists of the components like the manifold, catalytic converter, the pipes connecting the components, muffler and the tail pipe. A 3D model was created using Rhino to represent the exhaust system of the Dodge RAM automobile. Figure 5.9 shows the 3D model with all the exhaust system components along with the engine block and the floor pan.

During experimentation the muffler surface was observed to vary by 10 degree Celsius from the catalytic converter end to the tail pipe end. The muffler surface was assigned temperature curves accordingly. Environmental data was assigned to the model based on the weather file available. The simulation was done for a period of 12 minutes and the resulting simulation is shown in Figure 5.10 (a – d) and 5.11. The image is color coded based on the color scale shown in the image.

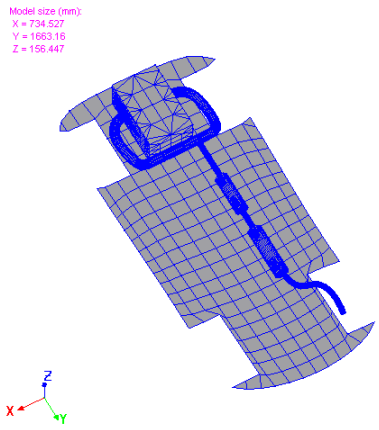

Figure 5-9 : Under vehicle chassis of the Dodge RAM 3500 vehicle.

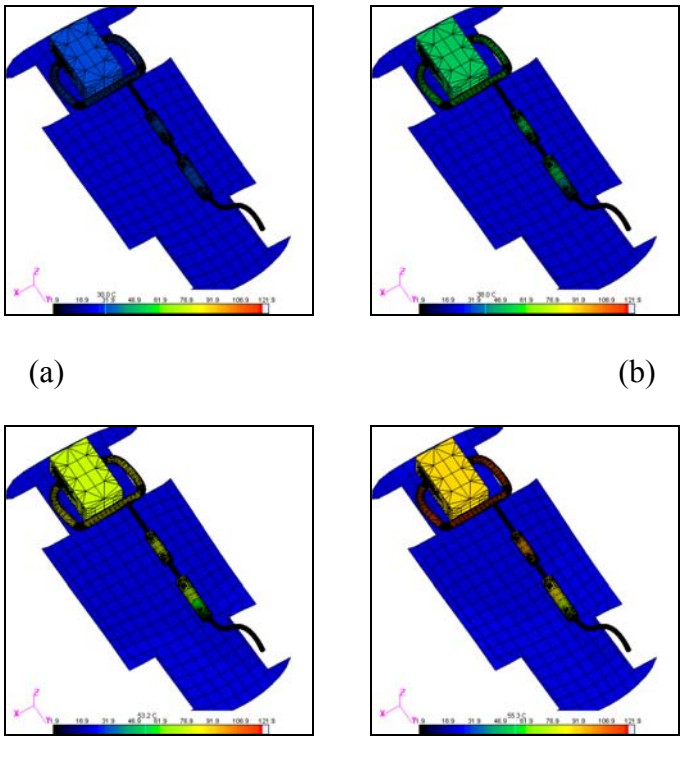

(a) (b)

(c) (d)

Figure 5-10: Simulated result of Dodge under vehicle chassis. (a) Simulation result at time 0 (b) Simulation result at 4 minutes (c) Simulation result at 8 minutes and (d) Simulation result at 12 minutes.

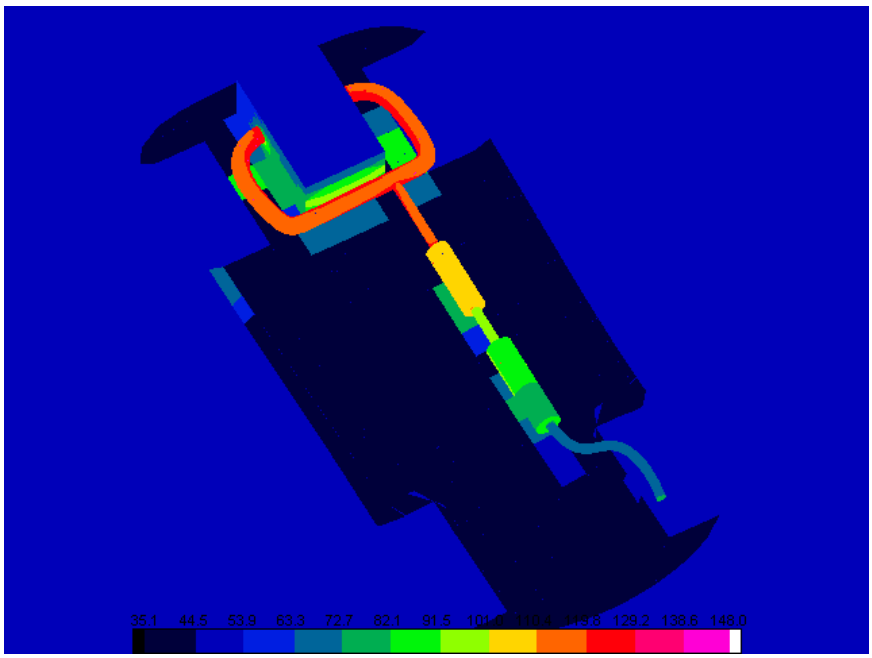

Figure 5-11: Simulation result of Dodge under vehicle chassis based on the acquired temperature data.

The 3D models and the results discussed so far were based on the self created models using 3D modeling tools. The models were of very low complexity and the simulation time taken was a maximum of 4 hours. The models are not close to real time as built automotive components. Modeling of as–built models requires professional expertise and it was not possible to include the exact shape using the 3D modeling tools. The CAD models were used for simulation of thermal images and the challenges and the results of simulation are discussed in the following section.

5.2 Simulation of CAD Models

The simulation results for the self created 3D models were shown and discussed in the previous section. As discussed earlier, for thermal modeling of as built automotive parts close to reality, it is necessary to use the exact 3D model similar to the real time vehicle. CAD models from the manufacturers are exact replica of the vehicle. This section deals

with the simulation of infrared images using the CAD model of the Toyota Tundra pick up truck.

Simulation of Thermal Model for Toyota Tundra CAD model

The visual image of the Toyota Tundra under vehicle chassis is shown in Figure 5.12(a) and the CAD model of the vehicle in Figure 5.12 (b). It can be inferred from the images that the CAD models are close to reality.

The Toyota Tundra model was purchased and downloaded from 3Dcad browser.com. The model was of high complexity and mesh was edited and cleaned to reduce the non significant components in the model. The exhaust system included various components such as catalytic converter, pipes, muffler and the heat shields. The complete drive train, including the gear box, transmission, drive shaft and the axle, was present in the model. Some parts are assigned as either calculated or assigned temperature parts as shown below.

1. Calculated temperature parts
   a. Drive shafts
   b. Steering
   c. Fan

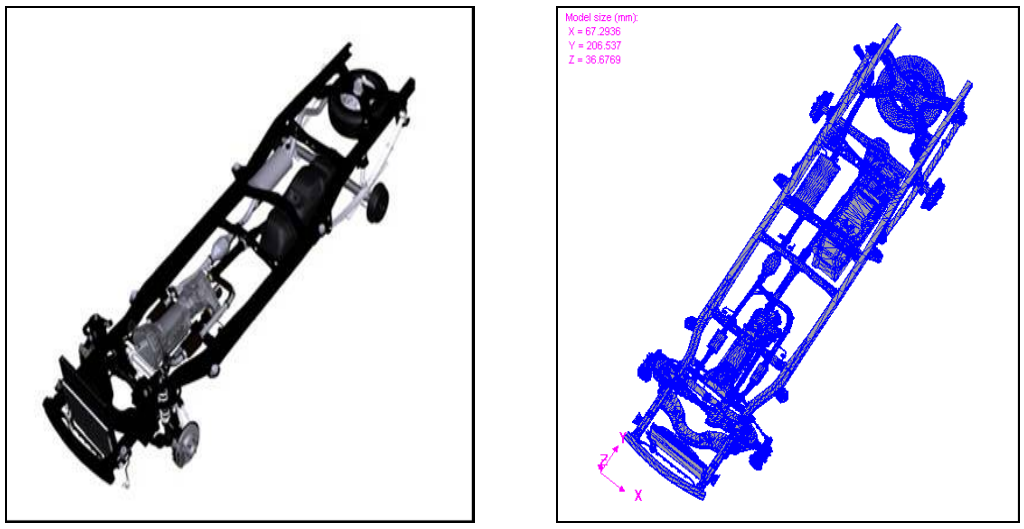

(a) (b)

Figure 5-12: Toyota Tundra under vehicle chassis (a) Visual image of the chassis (b) CAD model of the chassis.

2. Assigned Temperature part
   a. Muffler
   b. Catalytic converter
   c. Radiator
   d. Pipes
   e. Intake and Exhaust manifold
   f. Discs and Drums

The body frame of the model and the final model used for simulation is shown in Figure 5.13. The properties and the solution time are set accordingly as discussed in the previous sections. A weather data file is included for the simulation of the thermal image as seen through a sensor. The results were taken for a step size of 1 minute and the tolerance slope for the convergence of solution was 5 x 10^{-7}. The number of iterations used for the convergence was 850. The view factor rays were set to be in between the accurate and faster calculations. The weather data file used was for July 19, 1984. The time taken for simulation was close to 2 days, due to the complexity of the model, which is one of the disadvantages of using CAD models. The result of simulation for the Toyota tundra under carriage model is shown in Figure 5.14 (a – d).

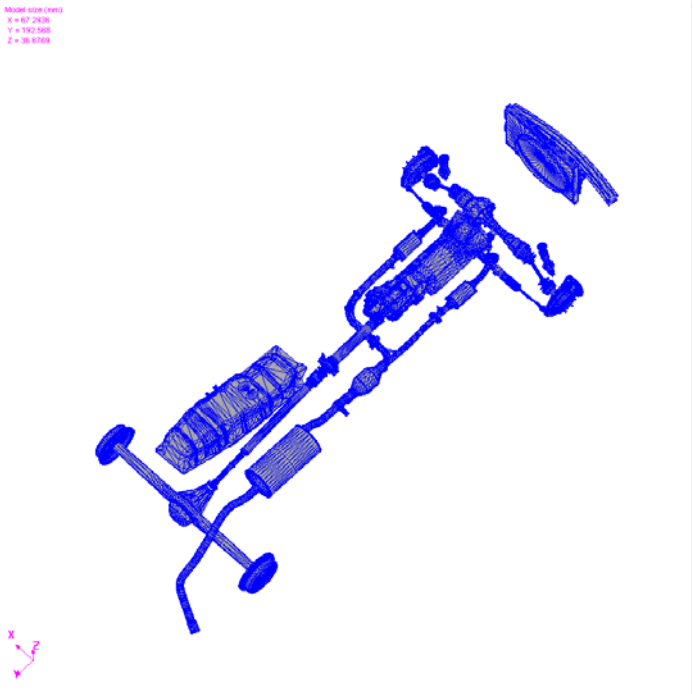

Figure 5-13: Original CAD model of the Toyota Tundra under carriage.

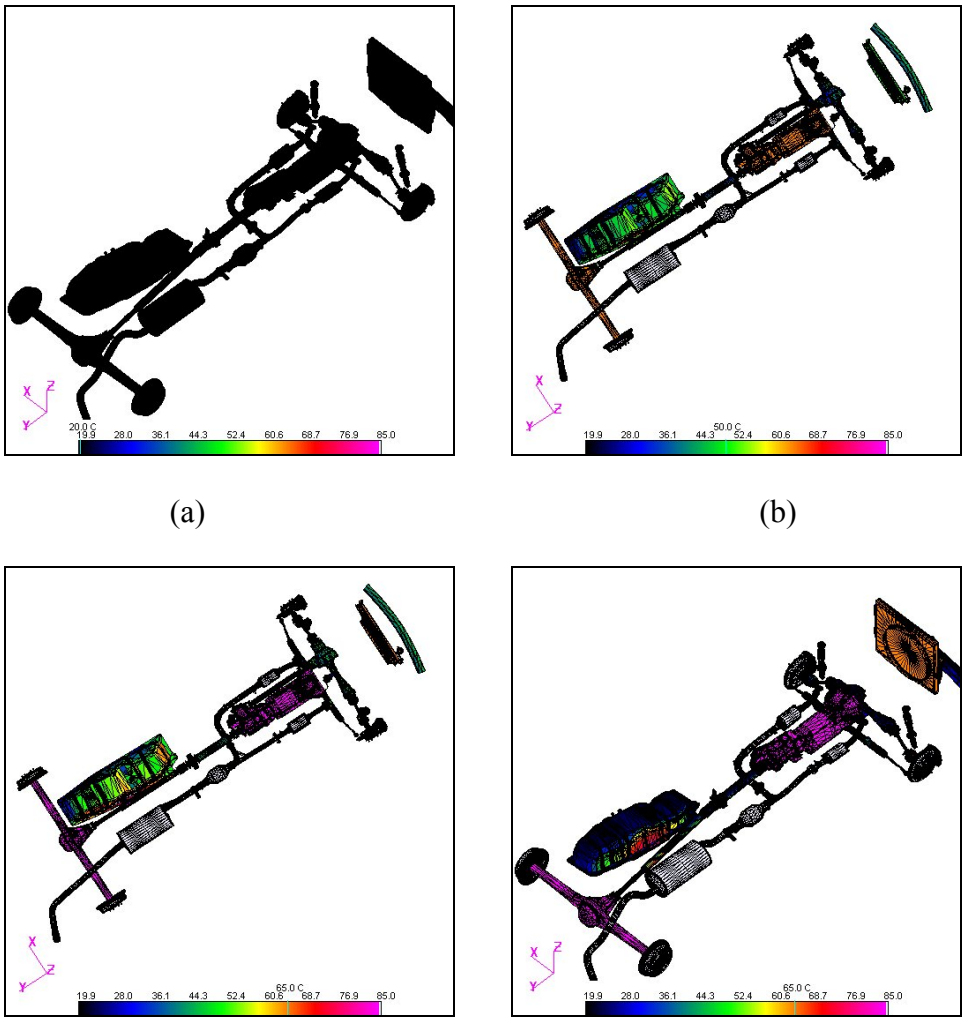

(a) (b)

© (d)

Figure 5-14: Simulated result of Toyota Tundra under vehicle chassis (a) Simulation result at time 0 (b) Simulation result at 5 minutes (c) Simulation result at 10 minutes and (d) Simulation result at 15 minutes.

In the figure, white represents high temperature and black represents cold regions. The exhaust system that is comprised of the catalytic converter, muffler and the pipes connecting the manifold and the muffler is at high temperature. The radiator, axle and differential are at a temperature based on the temperature curves assigned for them. Calculated temperature parts are assigned temperatures based on the numerical calculations. The convection assumed for the numerical solution is linear convection.

The simulated thermal image based on the bidirectional reflectance solution and the signature analysis is shown in Figure 5.15. The gas tank is at low temperature as expected and the exhaust system is at the high temperature. The rest of the under vehicle parts are at temperatures based on the curves assigned or based on the numerical calculation. Here white represents the highest temperature and black represents cold. The temperature of the exhaust system components was close to 350 degree Celsius, which is a reasonable value compared to real time temperature

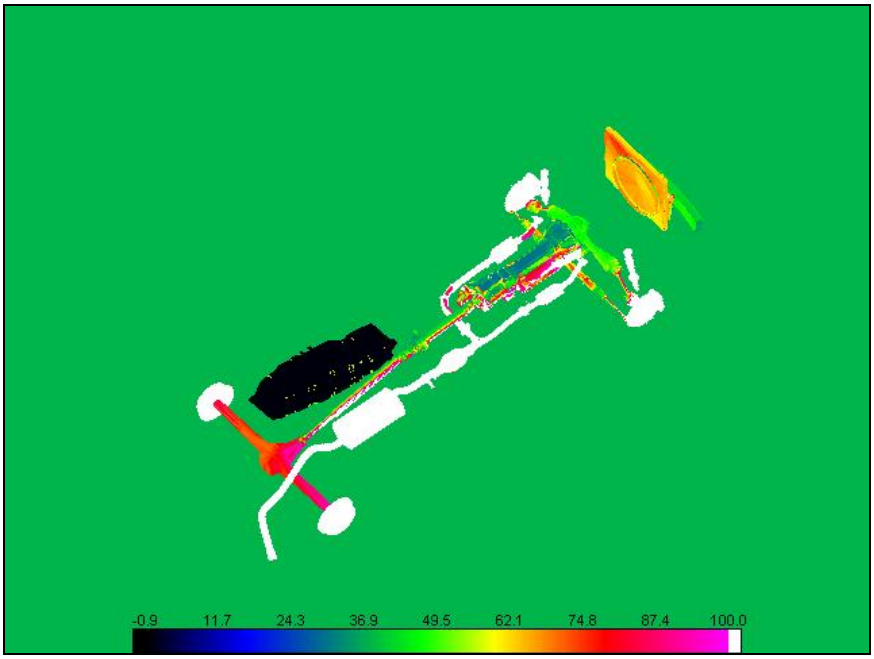

Figure 5-15: Simulated thermal image as seen through a sensor.

Simulation of Thermal Model for Toyota Tundra Engine model

In order to view the results of the complete vehicle, the engine block and the corresponding under the hood components were also simulated. The engine model, shown in Figure 5.16, was purchased and downloaded from www.3dcadbrowser.com. The engine model is an example of highly complicated model. The model consisted of 1104 parts initially and the number of elements was nearly 700,000. The model was then decomposed into individual VRML files and then they were grouped to form meaningful parts. The number of elements was reduced by using mesh reduction software and then the simulation was done for a period of 15 minutes. The temperature curves were assigned similar to the previous models and the final result of simulation is shown in Figure 5.17 (a –d).

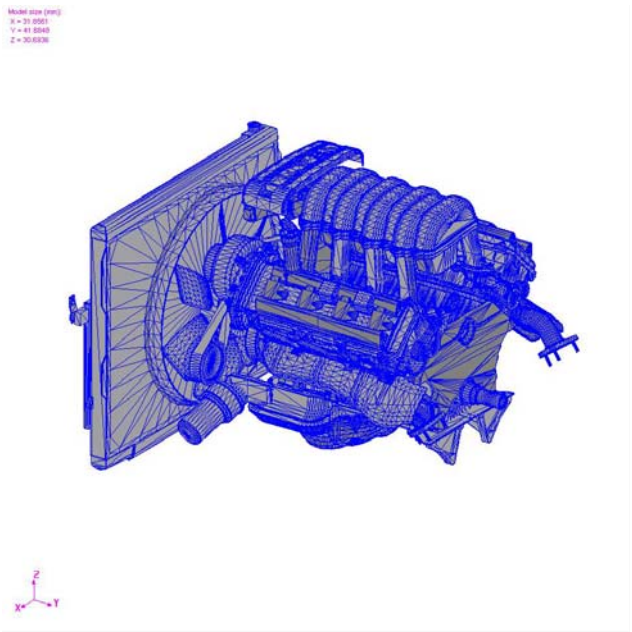

Figure 5-16: Original CAD model of the Toyota Tundra engine.

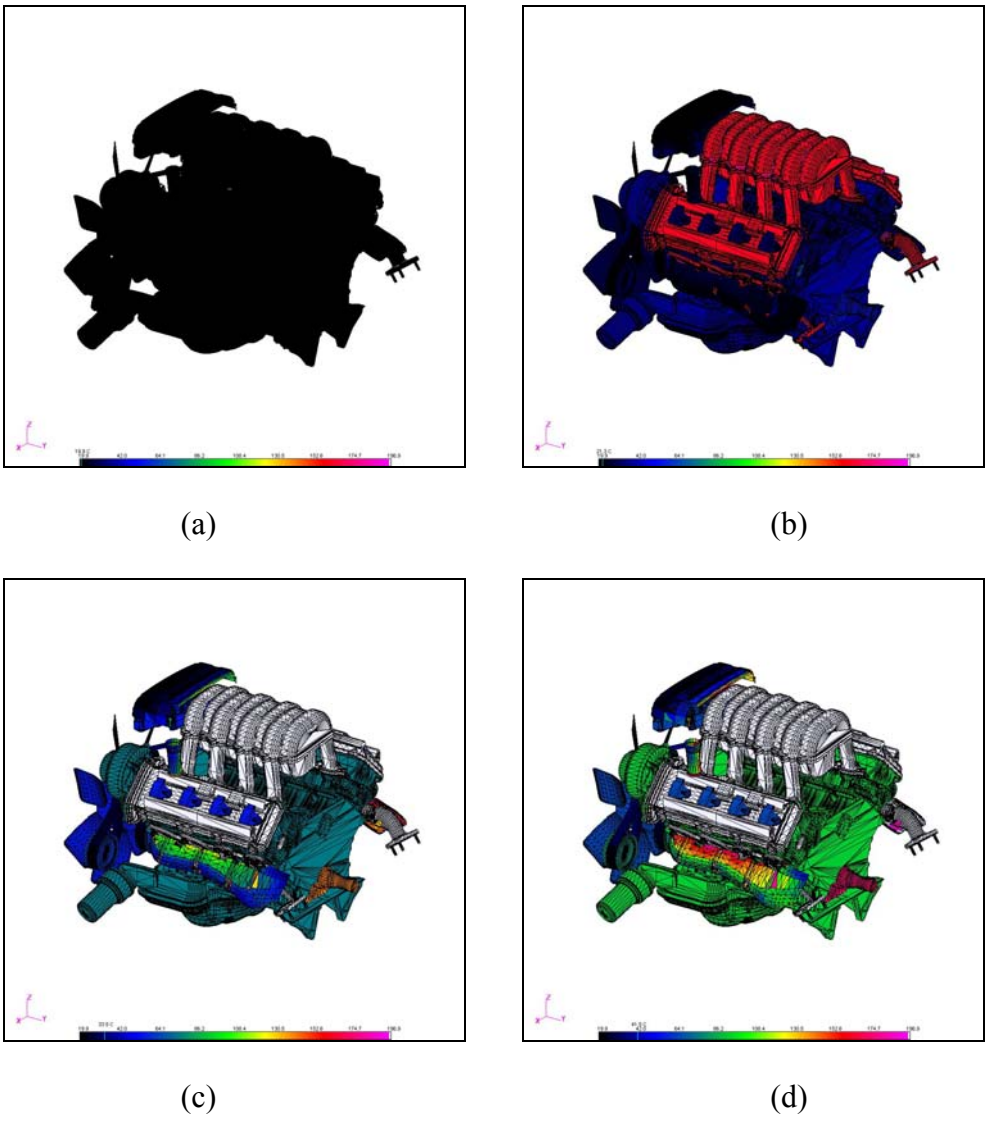

(a) (b)

(c) (d)

Figure 5-17: Simulated result of Toyota Tundra engine. (a) Simulation result at time 0 (b) Simulation result at 5 minutes (c) Simulation result at 10 minutes and (d) Simulation result at 15 minutes.

5.3 Simulation of Reverse Engineered Automotive Component

Thermal images of the under vehicle chassis of the Toyota Tundra vehicle was simulated using the CAD model. The results obtained were good, but the time taken for simulation was more due to the complexity of the CAD model used. Although the CAD models are close to reality and represent as built automotive components maintaining their shape and structure, cleaning up of the mesh and subsequent processing of the mesh takes almost weeks to produce an effective mesh for thermal modeling.

The CAD data is incomplete, meaning that the geometries of the components may intersect with each other and need to be trimmed. This adds to the burden of the CAD data cleaning process. Generally, a large number of CAD models are needed to create assemblies. For example, the engine typically is comprised of close to a hundred pieces that come together. This was intuitive from the CAD model of the Toyota Tundra engine discussed earlier. The detail in the CAD data is typically much more than what is needed for thermal modeling. Unnecessary details should be removed from the geometry which again must be done manually on a part by part basis.

The modeling of as built automotive components by avoiding CAD meshes was made successful by the concept of reverse engineering. Reverse engineering [Page et al., 2003] involves the process of range scanning the real automotive components in various views and registering them together to get a single view. The point clouds are extracted from that final single view and are triangulated to get a 3D mesh. The process of reverse engineering is shown in Figure 5.18 [Chidambaram, 2003]. The main advantage of this process is that the under hood/under vehicle components can be modeled as they are in the vehicle and is more close to reality. In our lab, the muffler was scanned use the range scanner and the multiple views were registered to form a single view and the final mesh was generated from the triangulation of the point clouds derived from the final view.

The 3D muffler model was a surface mesh which was then appended to the synthetic car under body model developed using Rhino. The thermal and boundary properties were assigned to the model based on the properties assigned to the complete car model in Section 5.1. The simulation was done for a period of 15 minutes. The original input model used for simulation is shown in Figure 5.19. The result of simulation is shown in Figure 5.20 (a – d). The muffler is close to reality and the exhaust system component is at higher temperature. The color scale is adjusted in such a way that the muffler variation is clearly seen. Similarly the other automotive components can be reversed engineered and the thermal modeling of such automotive components can be achieved. The experimental results for the thermal simulation of the under hood and under vehicle automotive components were shown and discussed in this section. The simulation can be more close to reality by incorporating the exact temperature predictions of the exhaust system or the internal heat transfer solutions. The next chapter discusses in detail the requirements for improved simulation and the ways of comparing between real and simulated thermal images.

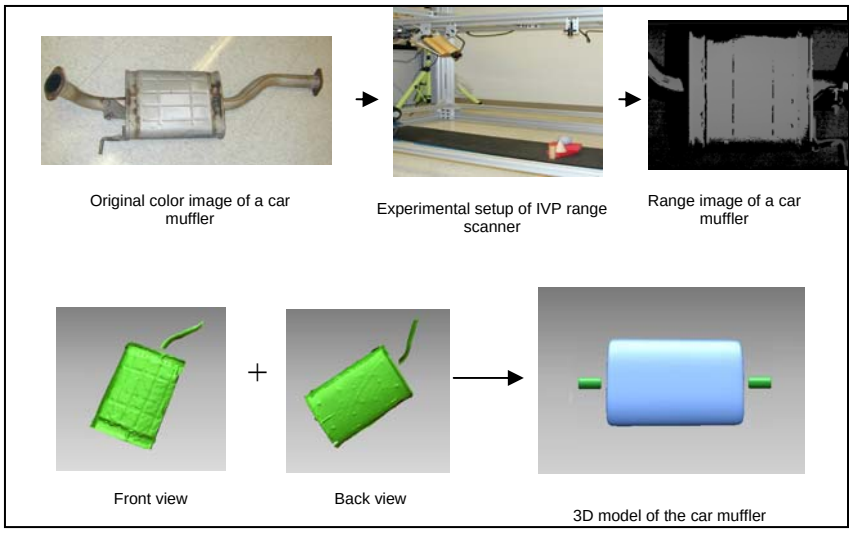

Figure 5-18: Concept of reverse engineering of automotive components [Chidambaram, 2003].

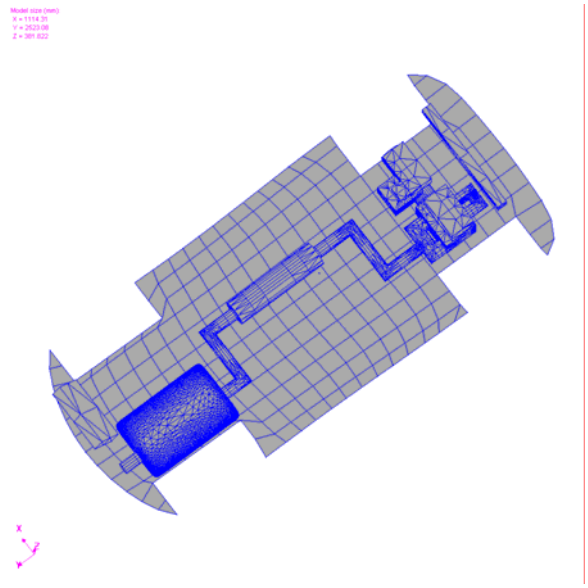

Figure 5-19: Synthetic CAD model of the car under body with the scanned muffler.

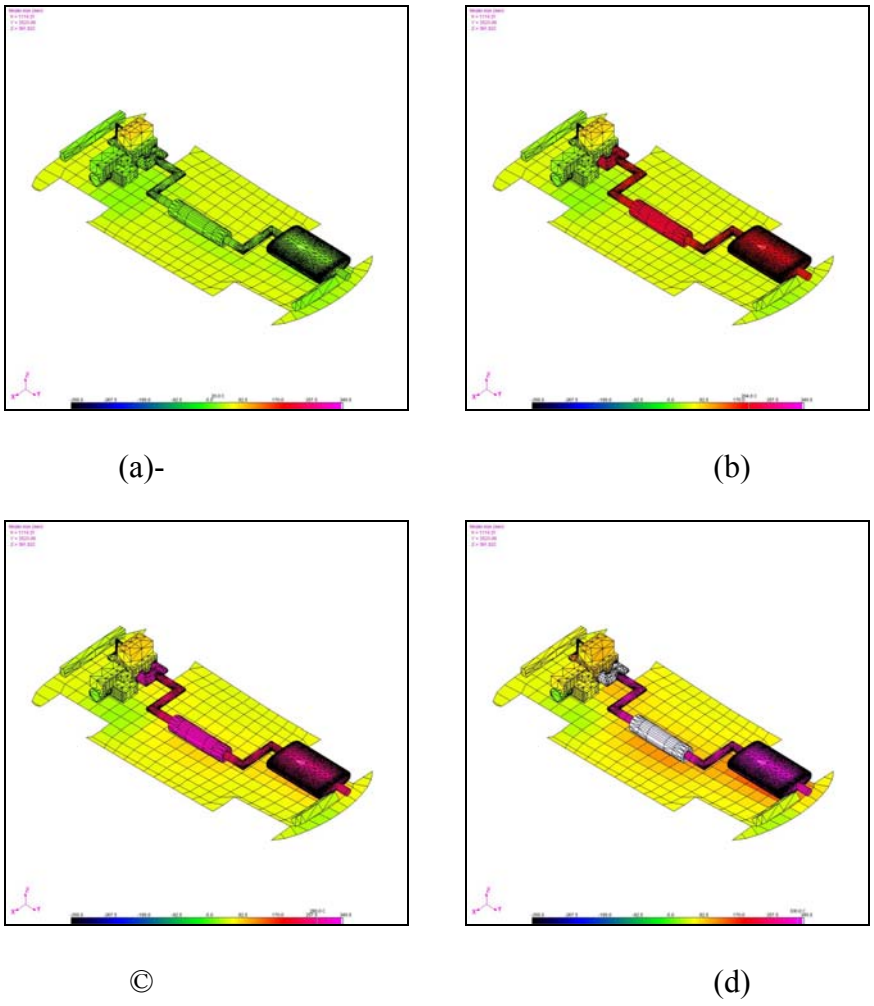

Figure 5-20: Simulated thermal model of the under vehicle chassis with reverse engineered muffler model (a) Simulation result at time 0 (b) Simulation result at 5 minutes (c) Simulation result at 10 minutes and (d) Simulation result at 15 minutes.

6 COMPARISON BETWEEN REAL AND SIMULATED THERMAL IMAGES

This chapter discusses the comparison between real and simulated thermal images. Section 6.1 describes the basic requirements of real and simulated thermal images in the context of comparison. Real thermal imaging effects and constraints are discussed in Section 6.2. The constraints in the synthesis of simulated thermal images are discussed in Section 6.3. Section 6.4 concludes with the limitations in thermal data acquisition and synthesis processes.

6.1 Real and Simulated Thermal Images

Real thermal images of automotive parts of under vehicle chassis show the heat distribution of the component under consideration. The heat radiations are captured with the help of the suitable sensor as discussed in the previous sections and the thermal images are acquired. Simulation of thermal images requires the knowledge of the radiation properties of the automotive parts and they are virtually synthesized to represent the real scene. There arises an argument – How close is this virtual simulation to reality? The solution for this argument can be achieved by comparing the real scene and the simulated scene and arriving at a conclusion which determines the percentage of similarity.

This section discusses in detail the idea of comparison and the basic things that has to be known about the real and simulated thermal images. Real thermal images can be acquired using an infrared sensor which is suitable for a particular application. The thermal camera used here for this purpose is the Indigo Omega thermal camera which was discussed earlier in the experimentation section. Simulated thermal images are synthesized using the simulation software for the exact conditions of the real thermal image. CAD models or LASER scanned and reconstructed model meshes are used for simulation of thermal images. Meshes were grouped into parts and thermal properties and bounding box conditions were assigned to 3D models in Chapter 5 and the thermal simulations were ran for a particular time period.

The following basic details should be approximately known from real thermal images of under vehicle automotive parts to simulate thermal images of the same component under consideration

1. Temperature curve of the component under consideration – For perfect simulation of an automotive component it is always necessary to know the temperature variations of the component with respect to time. The transient solution for the model can be done based on the temperature curve of the component over a specific period of time.

2. Effect of outside and inside geometry – The meshes used for simulation are usually surface meshes and actually there are no volumetric details available about the component under consideration. The muffler is a perfect example where the interior of the muffler tries to reduce the exhaust air pressure and as well as the temperature of the exhaust gas before it comes out.

3. Effect of Environmental Conditions – The climatic conditions affect the real thermal image obtained and it necessitates the knowledge of the environmental conditions for simulating a thermal model under the same conditions and also helps in comparison. The environmental data required are time, air temperature, wind direction, solar irradiance, wind speed, humidity, long wave infrared radiation, cloud cover and rain rate

4. Geometry of the component under consideration – For simulation of athermal image, it is necessary to have a thermal mesh exactly similar in geometry of the original component under consideration. This aids in visualization of the model both in reality and virtually. Meshes could be CAD meshes or LASER scanned and reconstructed.

5. Method of comparison – Acquire real thermal image, get the thermal properties of the parts, environmental properties, simulate thermal images based on the obtained data and finally approximate the resulting simulated thermal image as close as possible to reality.

6. Temperature Measurement – Infrared thermometer is used to measure the temperature changes of an automotive part with respect to time. The limitation is that the infrared thermometer measures only the surface temperature. The inside temperature of the automotive part cannot be measured and this is true with the thermal imaging devices. They are also able to see only the surface radiation. The inside effects cannot be avoided since the surface temperature varies based on the inside combustion or exhaust gas flow.

6.2 Real Thermal Images

Real thermal images are those that are acquired from real targets that radiate energy. For acquiring a real thermal image of an automotive part, it is necessary to build an

acquisition system which includes the thermal camera, the target and the blackbody calibrator for initial calibration.

1. Selection of a thermal IR camera:

   Selection of thermal camera plays an important role based on the type of application; it can either be a cooled camera for high precision applications or an uncooled camera with less sensitivity. The following points also aid to the selection of the suitable camera.

   - The range of temperatures to be imaged is the most fundamental parameter to identify.
   - The ability of the material's surface to emit thermal radiation, a property called *emissivity*, is usually a concern with glass, plastic, and other very shiny materials.
   - The surface must be viewable by direct line of sight, or obstructions will partially obscure the thermal image.
   - Transparency or opaqueness of the material in IR spectrum – an especially important consideration when you are measuring glass or plastic materials.
   - Size of the target when compared with the field of view of the camera. The target should be twice as large as the field of view in order to avoid the background scenes.
   - Environmental conditions like problems with smoke, dust, or other particulates in the measurement area. This adversely affects the thermal image quality or temperature measurement accuracy.
   - Requirements of the application's measurement/control interface. For example, the Indigo Omega camera can be controlled through the control panel software provided by the manufacturer, which results in the use of a laptop or PC and the necessary power requirements.
   - Resolution of the image also plays an important role in the selection of the thermal camera. For closely comparing the heat pattern of the automotive part in real and simulated thermal image high resolution images are better and provide much detail regarding the heat pattern.

2. Type of infrared camera

The under vehicle chassis automotive components show significant changes in their heat pattern. Real time thermal images are acquired with the help of infrared cameras either cooled or uncooled. Cooled thermal cameras are the best suited for such type of applications. They are more sensitive and can differentiate minute changes in temperature such as fraction of a degree whereas uncooled camera's output vary by ± 1 degree Celsius. For effective comparison exact temperature variations should be known.

3. Method of imaging

   Real thermal images of automotive component are acquired by running the vehicle and capturing the heat radiation emitted by the component with respect to time. All the components have to be mounted on the vehicle in order to emit heat radiations.

   Thermal images are acquired based on the field of view of the camera used, which results in several images of the whole under vehicle chassis. For simulations, a complete CAD model or reconstructed geometry is used to obtain the simulated thermal image. Hence, for comparing the real and simulated thermal images of the under vehicle chassis, it is necessary that the real images also represent the complete under vehicle chassis in one single image. Hence for the purpose of comparison, mosaicing of the real thermal images has to be done to form a single thermal image.

6.3 Simulated Thermal Images

Thermal images simulated using the same environmental conditions cannot be the same as the real thermal images of the automotive part. But comparison also means how close to reality we can simulate a thermal image of an automotive part. There are certain requirements or factors that govern the simulation of a thermal image

1. Thermal properties of the automotive part under consideration

   For simulating a thermal image of an automotive part or complete under vehicle chassis it is necessary to know the thermal properties of the part. The thermal properties are given by the

   i. Material properties of the part - This specifies the material density, thermal conductivity and specific heat of the particular material type used. This parameter is assigned for calculated thermal parts only. Based on the type of the material assigned, the numerical solution calculates the net energy incident on the element or part.

ii. Thickness of the part - The thickness value is used to determine the capacitance of the part and it is mainly used for conduction. It does not mean anything with the geometry used.

iii. Temperature curve - Initial temperature for the meshes is set to be the room temperature. A temperature curve has to be assigned at least to one part so that the other calculated parts are heated based on the radiation, conduction and convection from the assigned temperature part. For assigning a temperature curve to a particular part, the temperature variation of the part with respect to time has to be known. Since this plays a major role in the final simulation, the temperature variation with respect to time for a particular part is measured using an infrared thermometer

2. Type of convection

   The H Coefficient sets the convection coefficient of the gas or liquid surrounding the front and/or back side of a part. The front and back side can have an H coefficient set independent of each other. The H Coefficient can be set as a constant value or a time-dependent curve. It is necessary to know the convection coefficient to simulate a thermal image close to reality; it gives the air flow rate or the fluid flow rate.

3. Effect of fluids in real time

   In an automotive vehicle there are many fluids like coolant fluid, engine oil fluid etc., which reduces the friction between the parts and carries away most of the heat. This effect cannot be included exactly as it is in real time.

4. Closeness to real thermal image

   As discussed above it is not possible to incorporate all the thermal properties in to the simulation of thermal image. Hence the simulated thermal image will not be exactly the same as real thermal image of the same component taken under same settings. Our aim is to only measure the closeness of the simulated thermal image to real thermal image, simulated with the same thermal properties and environmental conditions.

6.4 Conclusion

Comparison between real and thermal images involves the complete knowledge of the temperature changes of the automotive part under consideration. There are some practical issues to be overcome in order to compare the two types of images. The best system to compare is the exhaust system of a vehicle with the simulated exhaust system. The

engine components are maintained at a certain temperature with the help of the coolant fluid, whereas the exhaust system is not internally forced to cool with the help of any coolant. The exhaust gas heats up the exhaust components as it passes through them. Commercial exhaust gas temperature monitors are available that can be used to measure the temperature changes with respect to time. Comparison of real and simulated thermal images is possible in the real sense only when all the details about the components are known and depends on the availability of similar CAD model.

7 CONCLUSIONS AND FUTURE WORK

Thermal images have a unique infrared prediction. The two types of thermal images, real and synthetic or simulated, provide information about the heat distribution in the object under consideration.

Real time images were acquired to serve as a basis for thermal modeling. They give an intuition about the heat pattern of the automotive component. It was observed that the exhaust system components are at higher temperatures compared with other parts. The measurement of temperature using the infrared thermometer served as a ground truth for simulation, which improves the simulation making it close to reality. The important application of thermal imaging in the field of threat detection was highlighted with the help of experiments.

Simulation of real time objects digitally helps in achieving time and cost reduction. Thermal modeling of as-built automotive parts was achieved successfully using the software MuSES. The modeling was done for meshes created using 3D modeling tools, CAD meshes from manufactures and reverse engineered automotive parts. Thermal modeling results can be improved by using 3D models which resemble the real automotive component. Meshing of the 3D meshes is an important factor which affects the simulation. The meshes should be as complete as possible without any missing elements. Exact temperature predictions of the automotive components will further improve the simulation. There is always a trade off between the complexity of the model and the memory requirement for processing and also the time taken for simulation.

Future work:

Thermal modeling of as built automotive parts was done based on the surface temperature measurements. Exact heat flow curves from the engine can be assigned to obtain simulation results close to reality. An infrared camera sees and records the surface temperature of the target and it is its limitation that the camera cannot exactly output what is taking place inside the component. There are certain parameters like the number of cylinders in the engine, capacity of the engine and others which affect the temperature of the exhaust gas and which in turn affects the temperatures of the exhaust system components. Knowledge of all such parameters can be incorporated into the simulation to get the thermal models and the thermal images close to reality.

Similarly the vehicle was run at idle during the experimental period and the temperature was recorded. Based on the experiments, the measured temperature was not same when the vehicle was running at idle and when the vehicle was running on a roadway. The measurement of exhaust gas temperature when the vehicle is running on a roadway can improve the simulation results, which exactly provides the real time temperature curve of the exhaust gas and not the surface temperature of the components.

Simulated thermal images of automotive components can be compared with real time images to obtain closeness to reality and they can serve as a database for comparing real time images for surveillance. Comparison of simulated thermal images with real time images poses several challenges all of which have to be overcome to achieve the objective of comparison. As discussed earlier, the geometry of the model used for simulation plays an important role in the final result of simulation. The model used should be an exact replica of the automotive components so that the visual comparison will be better. The temperature and thermal properties play an equally important role. The software should also be flexible enough to model all the heat flow properties and the conduction and convection parameters.

BIBLIOGRAPHY

Bajscy, P. and Saha, S., " A New Thermal Infrared Camera Calibration Approach using Wireless MEMS Sensors," *Proceedings of Communication Networks and Distributed Systems Modeling and Simulation Conference*, 2004.

Chevrette, P., "Calibration of Thermal Imagers," Proceedings *of the SPIE – The International Society for Optical Engineering,* 1986, Volume 661, pp. 372-382.

Chidambaram, U., "Edge Extraction of Color and Range Images," *Masters Thesis, Imaging Robotics and Intelligent Systems Laboratory, 2003.*

Curran, A. R., Johnson, K. R., Marttila, E. A., " Automated Radiation Modeling for Vehicle Thermal Management", *SAE International Congress and Exposition,* Detroit, Michigan, 1995

Dai, K, Li, X-X., and Shaw, L. L., "Comparisons between Thermal Modeling and Experiments: Effects of Substrate Preheating," *Rapid Prototyping Journal,* 2004, Volume 10, pp. 24-34.

Damodaran, V. and Kaushik, S., "Simulation to Identify and Resolve Under Hood/ Under Vehicle Thermal Issues," *Journal Articles by FLUENT Users*, 2000, pp. 1-4.

Dewitt, D. P., Nutter, G. D., Love, T. J., "*Theory and Practice of Radiation Thermometry,* " A Wiley Inter Science Publication, 1988.

Fox, N.P, Prior, T. R., and Theocharous, E., "Radiometric Calibration of Infrared Detectors and Thermal Imaging Systems," Proceedings *of the SPIE – The International Society for Optical Engineering*, 1995, Volume 2474, pp. 229-237.

Gambotto, J. P., "Combining Image Analysis and Thermal Models for Infrared Scene Simulations," *Proceedings of International Conference on Image Processing,* 1994, Volume 1, pp. 710-714.

Heijden, G.W.A.M. and Glasbey, C.A., "Calibrating Spectral Images using Penalized Likelihood," *Real time Imaging,* 2003, Volume 09, pp. 231-236.

Indigo Systems, http://www.indigosystems.com/product/omega.html

Jacobs, P. A., "*Thermal Infrared Characterization of Ground Targets and Backgrounds*," SPIE – The International Society for Optical Engineering, USA, 1996.

Johnson, K., Curran, A., Less, D., Levanen, D., and Marttila, E., "MuSES: A New Heat and Signature Management Design Tool for Virtual Prototyping," *Ninth Annual Ground Target Modeling and Validation Conference*, Houghton, Michigan, August 1998.

Johnson, K., Curran, A., Less, D., Levanen, D., and Marttila, E., "MuSES: A New Heat and Signature Management Design Tool for Virtual Prototyping (a follow-on)," *Tenth Annual Ground Target Modeling and Validation Conference*, Houghton, Michigan, August 1999.

Kaksonen, V., "Radiosity", *Seminar on Computer Graphics: Advanced Rendering Techniques,* Spring 2002.

Kaplan, H. and Scanlon, T., "A Thermographer's Guide to Infrared Detectors," http://www.flirthermography.com/media/14%20Kaplan%20Scanlon%202001.pdf

Ketkar, S. P., "*Numerical Thermal Analysis",* ASME Press, New York, 1999.

Lienhard IV, J. H. IV and Lienhard V, J. H., "*A Heat Transfer Textbook Third Edition",* Phlogiston Press, Massachusetts, 2004.

Merritt, T. P. and Hall, F.F, JR "Blackbody Radiation," Proceedings *of the SPIE – The International Society for Optical Engineering,* 1959, Volume 47, Issue 2, pp. 1435-1441.

Mermelstein, M. D., Snail, K.A., Priest, R. G., "Spectral and Radiometric Calibration of Midwave and Longwave Infrared Cameras," *Optical Engineering*, 2000, Volume 39, Issue 2, pp. 347-352.

Mitsunaga, T. and Nayar, S. K., "Radiometric Self Calibration," *Computer Vision and Pattern Recognition*, 1999, Volume 1, pp. 347-352.

Thermoanalytics Inc. www.thermoanalytics.com

Nicholas, J. V. and White, D. R., "*Traceable Temperatures: An Introduction to Temperature Measurement and Calibration,"* John Wiley and Sons, New York, USA, 1994.

Omega Engineering, http://www.omega.com/techref/iredtempmeasur.html

Page, D., Koschan, A., Sun, Y., and Abidi, M., "Laser-based Imaging for Reverse Engineering," *Sensor Review, Special issue on Machine Vision and Laser Scanners,* July 2003, Volume 23, Issue 3, pp. 223-229.

Parl, H. S., Dobie, D. W., Ferretta, T. E., Hakala, D. B., Noaln, M. P., Parker, E. L., "Radiometric Calibration System for Infrared Cameras," *Proceedings of SPIE - The International Society for Optical Engineering,* 1992, Volume 1686, pp. 35-45.

Quinn, T. J., "*Monographs in Physical Measurement: Temperature,"* Academic press, New York, USA, 1983.

Raytek Non Contact Temperature Measurement http://www.raytek.com

Raytheon http://www.raytheon.com

Spiro, I. J., *"Selected Papers on Radiometry,"* SPIE Milestone Series, SPIE- The International Society for Optical Engineering, USA, 1990, Volume MS14.

Srinivasan, K., Z. J. Wang, W. Yuan, R. Sun, " Vehicle Thermal Management Simulation using a Rapid Omni-Tree based Adaptive Cartesian Mesh Generation Methodology," *In the Proceedings of HTFED2004,* Charlotte, North Carolina, July 2004.

Wyatt, C. L., "Theory and Methods of Radiometric Calibration," Proceedings *of SPIE - The International Society for Optical Engineering,* 1976, Volume 95, pp. 217-222.

Xiao, Z., "A Hot Calibration Load for Measuring and Controlling Temperature," *International Journal of Infrared and Millimeter Waves,* 2000, Volume 21, Issue 7, pp. 1141-1151.

Xiao, Z., "Brightness Temperature Emitted by Radiometer Calibration Load at Millimeter Wave Band," *International Journal of Infrared and Millimeter Waves,* 2001, Volume 22, Issue 4, pp. 553-569.

Zissis, G. J., "Fundamentals of Infrared – A Review," *Proceedings of SPIE - The International Society for Optical Engineering,* 1975, Volume 62, pp. 67-95.

VITA

Vijaya Priya Muthusamy Govindasamy was born in Coimbatore, India on August 6th, 1980, the daughter of Dr. Govindasamy and Manimozhi, and is now the wife of Giri Palanisamy. She graduated with a Bachelors Degree in Electrical and Electronics Engineering from Bharathiyar University, Coimbatore, India in 2001. She came to US after her marriage in May 2002. With lots of encouragement and support from her husband, Giri, she pursued her graduate studies in the field of image processing at the Imaging, Robotics and Intelligent Systems Laboratory at the University of Tennessee, Knoxville.